

AP39 inhibits ferroptosis by inhibiting mitochondrial autophagy through the PINK1/parkin pathway to improve myocardial fibrosis with myocardial infarction

Ting Yang^{a,b,1}, Qi Yang^{c,1}, Qi Lai^{a,b}, Junxiong Zhao^c, Liangui Nie^c, Shengquan Liu^c, Jun Yang^{c,*}, Chun Chu^{a,**}

^a Department of Pharmacy, The Second Affiliated Hospital, Hengyang Medical School, University of South China, Hengyang 421000, Hunan Province, China

^b School of Pharmaceutical Science of University of South China, Hengyang 421000, Hunan Province, China

^c Department of Cardiology, The First Affiliated Hospital, Hengyang Medical School, University of South China, Hengyang 421000, Hunan Province, China

ARTICLE INFO

Keywords:

Hydrogen sulfide
AP39
Mitochondrial autophagy
Ferroptosis
Myocardial infarction
Myocardial fibrosis

ABSTRACT

Background and purpose: Research has revealed the involvement of mitochondrial autophagy and iron death in the pathogenesis of myocardial fibrosis. The objective of this study is to investigate whether the mitochondrial-targeted H₂S donor AP39 inhibits mitochondrial autophagy and antagonizes myocardial cell iron death through the PINK1/Parkin pathway, thereby improving myocardial fibrosis in rats with myocardial infarction.

Experimental approach: A rat model of myocardial infarction was created by intraperitoneal injection of a high dose of isoproterenol, and H9c2 myocardial cells were subjected to hypoxic injury induced by CoCl₂. Western blot, RT-PCR, transmission electron microscopy, immunohistochemistry, as well as echocardiography, and studies on isolated hearts were employed.

Key results: In the hearts of rats with myocardial infarction, there was a significant accumulation of interstitial collagen fibers, accompanied by downregulation of CSE protein expression, activation of the PINK1/Parkin signaling pathway, and activation of mitochondrial autophagy. Intervention with AP39 resulted in a significant improvement of the aforementioned changes, which could be reversed by the addition of PAG. Similar results were observed in vitro experiments. Furthermore, the addition of CCCP reversed the antagonistic effect of AP39 on myocardial cell iron death, while the addition of RSL3 reversed the inhibitory effect of AP39 on collagen production in myocardial cells.

Conclusion and implications: The mitochondrial-targeted H₂S donor AP39 can inhibit mitochondrial autophagy through the PINK1/Parkin pathway, antagonize myocardial cell iron death, and improve myocardial fibrosis in rats with myocardial infarction.

1. Introduction

Myocardial infarction (MI) is a cardiovascular disease characterized by sudden onset, severe symptoms, and high prevalence. Despite

significant advancements in modern medicine, the mortality rate after myocardial infarction remains high. It is estimated that approximately 17 million people worldwide die each year from acute myocardial infarction or its subsequent progressive heart failure, making it one of

Abbreviations: MI, myocardial infarction; ROS, reactive oxygen species; H₂S, hydrogen sulfide; ISO, Isoproterenol; ECG, electrocardiogram; cTnT, Troponin T; HR, heart rate; LVFS, left ventricular fractional shortening; LVEF, left ventricular ejection fraction; HW, heart weight; BW, body weight; PAG, dl-propargylglycine, CCCP, carbonyl cyanide-m-chlorophenyl-hydrazine; CSE, cystathionine gamma-lyase; PINK1, pten induced kinase 1; GPX4, glutathione peroxidase 4; SLC7A11, solute carrier family 7 member 11; TfRc, transferrin receptor.

* Correspondence to: Department of Cardiology, The First Affiliated Hospital, Hengyang Medical School, University of South China, No.69, Fengshan Avenue, Hengyang 421000, Hunan Province, China.

** Correspondence to: Department of Pharmacy, The Second Affiliated Hospital, Hengyang Medical School, University of South China, No.35 Jiefang Avenue, Hengyang 421000, Hunan Province, China.

E-mail addresses: yangjunktizu@163.com (J. Yang), 1996020012@usc.edu.cn (C. Chu).

¹ Contributed equally and share first authorship.

<https://doi.org/10.1016/j.bioph.2023.115195>

Received 6 June 2023; Received in revised form 10 July 2023; Accepted 18 July 2023

0753-3322/© 2023 The Authors. Published by Elsevier Masson SAS. This is an open access article under the CC BY-NC-ND license (<http://creativecommons.org/licenses/by-nc-nd/4.0/>).

the leading causes of death among Chinese residents [1]. Myocardial fibrosis is a crucial process in the development of myocardial remodeling and a primary pathological process following myocardial infarction. Excessive myocardial fibrosis and severe negative cardiac remodeling can lead to serious complications such as arrhythmias, hypotension, shock, and heart failure, significantly affecting the long-term prognosis of myocardial infarction patients. Therefore, exploring the mechanisms underlying its occurrence and development is of great scientific significance. Extensive research has identified several mechanisms involved in the development of myocardial fibrosis after myocardial infarction, including inflammation, oxidative stress, cell apoptosis, and cell pyroptosis [2–4]. Studies have proposed a close relationship between excessive mitochondrial autophagy, ferroptosis, and the occurrence of myocardial fibrosis [5], but the specific regulatory mechanisms remain unclear.

Mitochondrial autophagy is a selective self-degradation process of damaged or aging mitochondria, contributing to the maintenance of mitochondrial network integrity and homeostasis. However, mitochondrial autophagy has a dual effect. Studies have shown that moderate stimulation within a certain time frame enhances mitochondrial autophagy, thus maintaining the quantity and normal function of mitochondria. However, prolonged excessive mitochondrial autophagy inevitably leads to mitochondrial depletion, which affects mitochondrial energy metabolism, cellular homeostasis, and can even result in cell death [6]. It has also been suggested that excessive mitochondrial autophagy leads to the clearance of a large number of mitochondria, impairing cellular mitochondrial metabolism and rapidly increasing the levels of reactive oxygen species (ROS) such as superoxide. With the continuous release of a large amount of ROS, inflammation can be activated and amplified, leading to further mitochondrial and cellular damage, thus forming a vicious cycle and ultimately resulting in fibrosis [7]. Research has shown that inhibiting excessive mitochondrial autophagy can improve heart failure in rats after myocardial infarction [8]. PINK1, a mitochondria-targeted serine/threonine kinase, and Parkin, a cytoplasmic ubiquitin E3 ligase, are involved in mitochondrial autophagy when mitochondria are damaged. The loss of mitochondrial membrane potential leads to the accumulation of PINK1 in the outer mitochondrial membrane [9], and PINK1 mediates the phosphorylation of serine 65 (Ser65) in the ubiquitin-like domain of Parkin, activating and recruiting Parkin [9–11], thus inducing mitochondrial autophagy. It has been found that long non-coding RNA H19 can downregulate the PINK1/Parkin pathway, antagonizing excessive mitochondrial autophagy induced by palmitic acid, thereby improving mitochondrial respiration and ATP generation in myocardial cells [12]. Therefore, the mechanism of myocardial injury and fibrosis after myocardial infarction may be associated with excessive mitochondrial autophagy mediated by the PINK1/Parkin pathway.

Ferroptosis is a novel form of iron-dependent programmed cell death, distinct from apoptosis, necrosis, and autophagy, and characterized by iron overload and accumulation of lipid peroxides [13]. Recent studies have shown that ferroptosis is one of the important causes of myocardial injury induced by myocardial infarction [14,15]. It has been reported that ferroptosis is involved in the process of myocardial fibrosis. Zhang et al. [16] found that Elabela, a novel endogenous ligand of the apelin receptor, can antagonize Ang II-mediated ferroptosis in CMVECs by regulating the IL-6/STAT3/GPX4 signaling pathway, thereby improving cardiac remodeling and fibrosis. Quercetin can also improve myocardial fibrosis and cardiac dysfunction by alleviating doxorubicin-induced ferroptosis in cardiomyocytes [17]. Resveratrol can reduce myocardial damage by inhibiting ferroptosis, thereby improving myocardial fibrosis after myocardial infarction [18]. Ferristatin promotes the antioxidant capacity of cardiac fibroblasts, reduces ferroptosis, and improves ischemia/reperfusion-induced myocardial fibrosis [19]. Thus, ferroptosis is closely related to the mechanism of myocardial fibrosis, but whether myocardial cell ferroptosis is associated with excessive mitochondrial autophagy and mediates the

occurrence of myocardial fibrosis after ischemia is still unclear.

Hydrogen sulfide (H₂S) is a gasotransmitter discovered after CO and NO [20]. A large body of evidence suggests that H₂S is involved in the pathophysiological processes of cardiovascular diseases such as atherosclerosis, hypertension, angiogenesis, and myocardial infarction [21]. H₂S plays a cardiovascular protective role in the body and is associated with anti-inflammatory, antioxidant, anti-apoptotic, and antifibrotic effects [22]. Previous studies by our research group have found that the H₂S donor NaSH can improve myocardial fibrosis in rat models of hyperthyroidism [23] and diabetes [24]. However, whether it can antagonize myocardial fibrosis after myocardial infarction and whether its mechanism is related to the inhibition of excessive mitochondrial autophagy and ferroptosis are currently unclear. AP39 [(10-oxo-10-(4-(3-thioxo-3 H-1,2-dithiol-5yl) phenoxy)decyl) triphenylphosphonium bromide] is a mitochondria-targeted H₂S donor that releases H₂S specifically within the mitochondria to exert mitochondrial protective effects [25]. Studies have indicated that AP39 can exert cellular protective effects through antioxidant stress in ischemia/reperfusion injury [22,26,27]. Whether AP39 can inhibit excessive mitochondrial autophagy, counteract myocardial cell ferroptosis, and improve myocardial fibrosis after myocardial infarction is currently unclear. Therefore, this study aims to establish an acute myocardial infarction rat model and intervene with AP39 to investigate whether restoring mitochondrial H₂S homeostasis can improve myocardial fibrosis after myocardial infarction. Additionally, it aims to explore whether the mechanism involves the inhibition of excessive mitochondrial autophagy and suppression of myocardial cell ferroptosis, potentially discovering new intervention targets for preventing and treating myocardial fibrosis and cardiac remodeling after myocardial infarction.

2. Materials and methods

2.1. Reagents

The H9c2 cell line was obtained from ATCC (Manassas, VA, USA), CoCl₂, dl-propargylglycine (PAG) and Carbonyl cyanide-*m*-chlorophenyl-hydrazone (CCCP, C2759) were purchased from Sigma-Aldrich (St. Louis, MO, USA). Isoproterenol (ISO) was from Melone Pharmaceutical (Dalian, China). AP39 (HY-126124) and RSL3 were obtained from MCE. Antibodies against PINK1, Parkin, P62, LC3, α -SMA, CollagenI, CollagenIII, GPX4, SLC7a11, GAPDH and HRP-conjugated anti-rabbit IgG secondary antibodies were all from Proteintech (Wuhan, China). Pierce Detergent Compatible Bradford Assay Reagent was purchased from thermo scientific (Rockford, USA). Enhanced Chemiluminescence Reagent kit was purchased from NCM Biotech (Suzhou, China). Reactive oxygen species assay kit and Enhanced mitochondrial membrane potential assay kit (JC-1) were obtained from Beyotime Institute of Biotechnology (Shanghai, China). Two-photon (TP) fluorescent probe Mito-HS was obtained KEAN Biotechnology (Nanjing, China).

2.2. Cell culture and treatment

The myocardial cell line H9c2 was bought from ATCC (Manassas, VA, USA). Cells were developed in the mixture of Dulbecco's Modified Eagle Medium (D-MEM) (C11995500BT; Gibco; Grand Island, NY, USA) which contains 10% fetal bovine serum (FSP500; Excell Bio; Uruguay, South America) under the condition of humidified 5% CO₂ and 37 °C. The Primary Rat Cardiomyocyte was bought from MeisenCTCC (CTCC-C002-Rat; Zhejiang; China). Cells were developed in the Cardiomyocyte complete medium (CTCC-022-PriMed; Zhejiang; China) under the condition of humidified 5% CO₂ and 37 °C.

Cells were disposed by trypsin/EDTA (BL512A; biosharp; Beijing, China) for subcultivation. The medium was replaced every other day.

H9c2 cells (100 μ l/well) were seeded into 96-well plate at a density of 3.0×10^4 cells/ml and incubated for 24 h in medium containing

different concentrations (0, 200, 400, 600, 800, 1000, 1200, 1400 and 1600 μM) of Cobalt chloride (CoCl_2 , Sigma-Aldrich, USA). Cell viability was tested with cell counting kit-8, the concentration of CoCl_2 resulting in half reduction of the cell viability was chosen to induce chemical hypoxia [28]. H9c2 cells were seeded at a density of 1×10^3 cells/well in 6-well culture dishes and cultured in standard DMEM supplemented with 10% calf serum at 37 °C in an incubator with humidified 5% CO_2 and 95% air atmosphere. When the cells reached ~60% confluence, 800 μM CoCl_2 was used to induce hypoxia. Groups were set up as following. Control group: H9c2 cardiomyocytes were cultured in a 5% CO_2 incubator at 37 °C for 48 h. CoCl_2 group (800 μM): diluted CoCl_2 was added, and after 24 h the culture medium was changed and cultured for another 24 h. CoCl_2 + AP39 group: diluted CoCl_2 was added and cultured for 24 h, then the medium was changed and AP39 (100 nM) was added and cultured for another 24 h. CoCl_2 + AP39 + PAG group: diluted CoCl_2 was added and cultured for 24 h, PAG was added half an hour before addition of AP39 and then co-cultured for another 24 h. CoCl_2 + AP39 + CCCP group: Carbonyl cyanide-m-chlorophenyl-hydrazine (C2759; Sigma-Aldrich; Merck KGaA, Darmstadt, Germany) was used to activate mitophagy in CCCP group. CoCl_2 + AP39 + RSL3 group: RSL3 ((1 S,3 R)-RSL3) (HY-100218A; Med Chem Express; New Jersey, USA) was used to activate ferroptosis. AP39 group: AP39(100 nM) was added to H9c2 cardiomyocytes and cultured for 48 h at 37 °C in a 5% CO_2 incubator. DMSO group: DMSO(2ul/well) was added to H9c2 cardiomyocytes and cultured for 48 h at 37 °C in a 5% CO_2 incubator.

The primary Rat Cardiomyocytes were seeded at a density of 5×10^5 cells/well in 6-well culture dishes and cultured in standard Cardiomyocyte complete medium supplemented with 10% calf serum at 37 °C in an incubator with humidified 5% CO_2 and 95% air atmosphere. When the cells are apposed for 12 h, 800 μM CoCl_2 was used to induce hypoxia. Groups were set up as following. Control group: primary Rat Cardiomyocytes were cultured in a 5% CO_2 incubator at 37 °C for 48 h. CoCl_2 group (800 μM): diluted CoCl_2 was added, and after 24 h the culture medium was changed and cultured for another 24 h. CoCl_2 + AP39 group: diluted CoCl_2 was added and cultured for 24 h, then the medium was changed and AP39 (100 nM) was added and cultured for another 24 h. CoCl_2 + AP39 + PAG group: diluted CoCl_2 was added and cultured for 24 h, PAG was added half an hour before addition of AP39 and then co-cultured for another 24 h. AP39 group: AP39(100 nM) was added to H9c2 cardiomyocytes and cultured for 48 h at 37 °C in a 5% CO_2 incubator.

2.3. Animals

Fifty adult male SD rats, weighing (220 ± 20 g), from the Animal Laboratory of South China University. This study was performed in accordance with the National Institutes of Health Guide for the Care and Use of Laboratory Animals. The experimental protocol was approved by the Animal Ethics Committee of the University of South China (USC202011SD25).

Fifty male SD rats were randomly divided into the following five groups: control group, ISO group (myocardial infarction rat group), ISO+AP39 group, ISO+AP39 +PAG group and AP39 group (n = 10). A rat model of myocardial ischemia was induced by intraperitoneal injection of ISO hydrochloride (50 mg/kg/d) for 2 consecutive days, while Control group and AP39 group were injected with normal saline for 2 consecutive days. And 24 h after the second ISO injection, all animals were anesthetized and electrodes are first separately implanted into the appropriate body part, and then the electrocardiogram (ECG) was monitored. Then, blood samples (2 ml) were collected from all rats through the tail vein, and serum was separated from each sample for biochemical analysis. Both the ISO+AP39, ISO+AP39 +PAG and AP39 groups were administered intraperitoneally with AP39. The ISO+AP39 +PAG group was given an additional intraperitoneal injection of CSE inhibitor PAG (dl-propargylglycine, 40 mg/kg/d, Sigma-Aldrich, USA). Intraperitoneal injections were performed continuously for 4 weeks.

2.4. Electrocardiography

Each group of rats underwent ECG before the first injection of ISO or saline and after the last injection (VECG-2303B, 3ray, Guangzhou, China). Fifteen minutes after anesthesia, SD rats were placed on a wooden board in the supine position, and red wire electrodes were bound to the paw pad of the right upper limb, yellow wire electrodes were bound to the paw pad of the left upper limb, green wire electrodes were bound to the paw pad of the left lower limb, and black wire electrodes were bound to the paw pad of the right lower limb, and the speed of the electrocardiograph was 50 mm/s. Subsequently, the electrocardiogram graphs were recorded and analyzed.

2.5. Troponin T (cTnT)

Blood was collected using heparin tubes immediately after execution of the rats, and blood samples were centrifuged at 12,000 rpm for 10 min at 4 °C using a high-speed cooling centrifuge, and then the supernatant was collected. The level of cTnT was then measured according to the instructions for the Troponin T (cTnT) assay kit.

2.6. Echocardiography

After all rats were anesthetized, the changes of Heart rate (HR), left ventricular fractional shortening (LVFS), and Left ventricular ejection fraction (LVEF) values were measured using M-mode ultrasound.

2.7. Measurement of cardiac index

After detection of cardiac function, the rats were sacrificed, then the hearts were removed and weighed. The heart mass index was calculated by ratio of heart weight (HW) and body weight (BW).

2.8. Masson staining

Myocardial tissues were fixed by 4% paraformaldehyde, paraffin-embedded after dehydration by gradient alcohol, made into 4 μm thin sections by microtome, stained according to the instructions of Masson staining kit (Abiowell Biotech Co, Ltd, Changsha, Hunan), sealed by treacle, and observed staining under a light microscope.

2.9. Immunohistochemistry analysis

The myocardial tissue was fixed in 4% paraformaldehyde saline and then rinsed with 100%, 95%, 85%, and 75% ethanol in sequence for 5 min. Tissues were soaked with PBS solution for ~5 min and incubated in 3% H_2O_2 for 10 min. Tissues were rinsed with PBS for three times (2 min for each time) and then incubated with the primary antibody overnight at 4 °C. After three times of wash with PBS (2 min for each time), tissues were incubated with biotin-labeled secondary antibody (Proteintech, Wuhan, China) for 10 ~ 30 min, followed by incubation with HRP-labeled streptavidin for 30 min. After extensive wash with PBS, samples were developed using 3,3'-diaminobenzidine (DAB) chromogen and observed under a Motic BA210T light microscope.

2.10. Transmission electron microscopy

Myocardial tissues were fixed with 2.5% glutaraldehyde, cut into 50–100 nm thin slices, and rinsed with phosphoric acid (Beyotime Institute of Biotechnology, Shanghai, China). After fixed immersion in 1% osmium tetroxide (Absin Biosciences, Inc, Shanghai, China), phosphoric acid was rinsed, followed by gradient acetone immersion, dehydration, and drying, staining with 3% uranyl acetate and lead nitrate for 10–20 min, rinsing with distilled water, and observation of ultrastructure under transmission electron microscopy.

2.11. Mito-HS fluorescent probe

Sterile coverslips were placed in each well of the six-well plate before seeding, and at the end of the cell intervention time, cells in each well were washed 3 times for 3 min each using PBS, the Mito-HS fluorescent probe [29] was added after aspiration of PBS and incubated for 1 h at 37 °C, and then the cells in the six-well plate were washed three times using PBS for 3 min each time. Finally, observation was made under fluorescence microscope.

2.12. Cell Counting kit-8 (CCK8)

The cell counting kit-8 (CCK-8) (Abiowell, AWC0114a, Changsha, China) assay was used to determine cell viability. H9c2 cells were first cultured in 96-well plates at a density of 1×10^4 cells/well. After respective treatments, 10 μ l of CCK-8 reagent was added to each well containing H9c2 cells. The plates were then incubated at 37 °C for 2 h in the dark. Each well's optical density (OD) was measured using an enzyme-labeled instrument at a wavelength of 450 nm.

2.13. JC-1 mitochondrial membrane potential measurement

Mitochondrial membrane potential changes in H9c2 cells and primary rat cardiomyocytes were measured by JC-1 kit (Beyotime Institute of Biotechnology, Shanghai, China). Briefly, H9c2 cells and primary rat cardiomyocytes were treated as described previously for modeling, and then H9c2 cells and primary rat cardiomyocytes were incubated with JC-1 staining solution (10 μ g/ml) for 20 min at 37 °C in the dark and rinsed twice with PBS, and images were taken under fluorescence microscope. The ratio of red fluorescence to green fluorescence reflects the change in mitochondrial membrane potential.

2.14. ROS detection assay

The cellular reactive oxygen species (ROS) assay is performed according to the manufacturer's instructions (S0033S). The ROS assay kit is based on the diffusion of 2',7'-dichlorofluorescein diacetate (DCFH-DA) into the cells. It is then deacetylated by the cell's esterase, and the product is subsequently oxidized by ROS to 2',7'-dichlorofluorescein (DCF), which is highly fluorescent. To detect intracellular ROS, post-intervention cells were incubated with 10 μ M DCFH-DA for 30 min at 37 °C. After that, the cells were washed with PBS 3 times, and images were taken under fluorescence microscope.

2.15. Mito-ferrogreen detection assay

The Fe^{2+} content of different groups was analyzed using a Mito-Ferrogreen Assay Kit (Dojindo, Shanghai, China) according to the manufacturer's instructions. The Fe^{2+} positive cells were green under fluorescence microscopy.

2.16. Immunofluorescence staining

Cells were fixed with 4% PFA for 40 min, permeabilized with 0.1% Triton X-100 for 5 min \times 2, and blocked with 5% BSA for 1 h, incubated with rabbit anti-PINK1 (1:100) overnight at 4 °C, then incubated with secondary antibody coupled with FITC (1:200) for 1 h at room temperature, followed by incubation with rabbit anti-Parkin (1:100) at 4 °C overnight, followed by incubation with a secondary antibody coupled with Cy3 (1:200) for 1 h at room temperature, and finally re-stained using DAPI. Fluorescence was analyzed using a fluorescence microscope (Olympus, IX71, Tokyo, Japan).

2.17. RT-qPCR

Total RNA was extracted from rat myocardial tissues using TRIzol

(Tiangen, China) and transcribed into cDNA using the Prime-ScriptTM RT kit (CWBio, China). Real-time qPCR was performed using SYBR green (CWBio, China) at standard conditions of 95 °C for 30 s, 40 cycles of 95 °C for 5 s, and 60 °C 30 s. Real-time qPCR was performed under standard conditions, GAPDH was used as an internal reference and the relative expression levels of target genes were calculated using the $2^{-\Delta\Delta Ct}$ method. The primer sequences were as follows:

R-GAPDH.
F ACAGCAACAGGGTGGTGGAC.
R TTTGAGGGTGCAGCGAACTT.
R-PINK1.
F GTGTCTGACCCACTGGACAC.
R CTGCTCCCTTTGAGACGACA.
R-P62.
F AGCATACAGAGAGCACCAT.
R ACATACAGAAGCCAGAATGCAG.
R-GPX4.
F AATTCGCAGCCAAGGACATCG.
R ATTGCTAAACCACACTCGGCGTA.
R-SLC7A11.
F TGCTGCCTACACAAAGACGTT.
R CGCCTTGCCCTTTAAGTATTCACC.

2.18. Western blotting

Rat myocardial tissues and cell precipitates were lysed using cold protease inhibitor-containing radioimmunoprecipitation assay (RIPA) lysis buffer, the supernatant was collected after centrifugation, and the protein concentration of the supernatant was quantified and leveled using the BCA protein quantification kit according to the manufacturer's guidelines, and samples were denatured after heating at 95 °C for 10 min, separated in 10–12% polyacrylamide electrophoresis gels, and electrophoretically transferred to a PVDF membrane (Polyvinylidene Fluoride Membrane, Millipore, USA). The membranes were blocked with 5% skim milk at RT for 1 h, followed by primary antibody at 4 °C overnight. The membranes were washed three times (5 min \times 3) with tris-buffered saline (TBST) containing Tween 20 and incubated with the corresponding species of horseradish peroxidase (HRP)-conjugated secondary antibody at RT for 1 h. After TBST washing (5 min \times 3), exposure shots were taken with ECL chemiluminescent solution, and image signals were acquired using the BIO-RAD XRS+ imaging system, and ImageJ software was used to analyze the relative data.

2.19. Statistical analysis

All values are expressed as the mean \pm standard error. Student's t test was performed with GraphPad Prism software (San Diego, California) to evaluate statistical significance and one-way analysis of variance (ANOVA) was used to analyze comparisons among multiple groups. But when there are two variables, we use two-way ANOVA. When $P < 0.05$, it is considered to be statistically significant. The data are statistically evaluated by variance analysis, and then Prism is used for Tukey post-test of inter-group comparison.

3. Result

3.1. Changes in cardiac troponin T levels among the groups of rats

In this experiment, the success of rat modeling was evaluated by measuring the changes in serum cardiac troponin T levels after intraperitoneal injection of ISO (50 mg/kg/d) for 2 days in the different groups of rats. A total of 30 rats were used to construct the myocardial infarction model, and 21 survived, with a mortality rate of 23.3%. Compared to the Control group, the levels of cardiac troponin T were significantly increased in the ISO group, AP39 +ISO group, and AP39 +ISO+PAG group, indicating the successful establishment of an acute

myocardial infarction rat model. However, there were no significant changes in cardiac troponin T levels in the AP39 group compared to the Control group. (Table 1).

3.2. Changes in electrocardiogram (ECG) in each group of rats

After the continuous intraperitoneal injection of a high dose of isoproterenol for 2 days to induce myocardial infarction in rats, ECG was performed on rats from each group. The results showed that the ECG of rats in the Control group and AP39 group exhibited a normal pattern. However, rats in the ISO group, AP39 +ISO group, and AP39 +ISO+PAG group displayed significant ST-segment elevation on lead II of the ECG, indicating the successful establishment of acute myocardial infarction rat models in the ISO group, AP39 +ISO group, and AP39 +ISO+PAG group (Fig. 1).

3.3. AP39 improves cardiac function and myocardial remodeling in rats with myocardial infarction

After 4 weeks of AP39 intervention, compared to the Control group, the HW (heart weight) and BW (body weight) were increased, and the HW/BW ratio was also increased ($P < 0.05$). In comparison to the ISO group, rats in the AP39 +ISO group showed decreased HW, BW, and HW/BW ratio ($P < 0.05$). However, in the AP39 +ISO+PAG group, the HW, BW, and HW/BW ratio were significantly increased compared to the AP39 +ISO group ($P < 0.05$) (Table 2).

Simultaneously, the rat echocardiography results showed that compared to the Control group, the ISO group had increased LVESD and LVEDD, and decreased FS ($P < 0.05$). In comparison to the ISO group, rats in the AP39 +ISO group exhibited decreased LVESD and LVEDD, and increased FS ($P < 0.05$). However, when compared to the AP39 +ISO group, rats in the AP39 +ISO+PAG group showed increased LVESD and LVEDD, and decreased FS ($P < 0.05$). There were no significant differences in the aforementioned parameters between the Control group and the AP39 group ($P > 0.05$) (Fig. 2; Table 3).

3.4. AP39 improves myocardial fibrosis in rats with myocardial infarction

To observe the degree of myocardial fibrosis in each group of rats, Masson's staining was performed in this experiment (Fig. 3A, F). The results showed that compared to the Control group, the ISO group exhibited significantly increased and disorganized blue-stained collagen deposition. In the AP39 +ISO group, the deposition of collagen fibers mentioned above was reduced compared to the ISO group. In comparison to the AP39 +ISO group, the AP39 +ISO+PAG group showed a significant increase in collagen fiber deposition. There was no significant difference in myocardial collagen deposition between the AP39 +ISO+PAG group and the ISO group. Moreover, no significant difference in myocardial collagen fiber deposition was observed between the AP39 group and the Control group. Immunohistochemical staining was performed to assess the expression of Collagen III protein in the myocardial tissue of each group of rats (Fig. 3B, G). Additionally, Western blotting experiments were conducted to examine the expression levels of fibrosis-related proteins such as Collagen III and α -SMA in the rat myocardial tissue (Fig. 3C-E). The results showed increased

Table 1

Expression of cardiac troponin T in each group (mean \pm SD).

Groups	number	cTnT (pg/ml)
Control	10	20.89 \pm 7.66
ISO	7	473.74 \pm 72.30*
AP39 +ISO	7	436.60 \pm 56.63 [#]
AP39 +ISO+PAG	7	426.69 \pm 37.08 [§]
AP39	10	24.36 \pm 9.45

Note: * $P < 0.05$, vs Control; [#] $P < 0.05$, vs Control; [§] $P < 0.05$, vs Control.

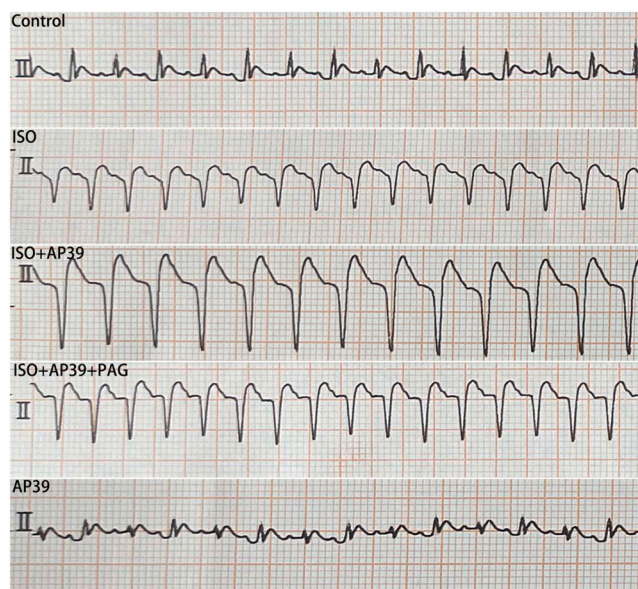


Fig. 1. Electrocardiogram (ECG) of rats in each group.

Table 2

Comparison of HW values, BW values, and HW/BW ratios among groups (mean \pm SD).

Groups	HW (mg)	BW (g)	HW/BW (mg/g)
Control	560.5 \pm 38.988	237.6 \pm 7.088	2.358 \pm 0.127
ISO	808.0 \pm 20.563 *	313.7 \pm 12.372*	2.578 \pm 0.075*
AP39 +ISO	543.9 \pm 31.092 [#]	245.0 \pm 12.000 [#]	2.222 \pm 0.106 [#]
AP39 +ISO+PAG	847.4 \pm 48.216 [§]	323.9 \pm 17.447 [§]	2.622 \pm 0.179 [§]
AP39	545.8 \pm 38.455	263.9 \pm 21.016	2.077 \pm 0.176

Note: * $P < 0.05$, vs Control; [#] $P < 0.05$, vs ISO; [§] $P < 0.05$, vs AP39 +ISO.

expression of the aforementioned proteins in the ISO group compared to the Control group ($P < 0.05$). After the AP39 intervention, the expression of these fibrosis-related proteins was significantly reduced ($P < 0.05$). However, simultaneous administration of the endogenous hydrogen sulfide synthase inhibitor PAG reversed these changes ($P < 0.05$). No statistically significant differences were observed in the expression of the above proteins in myocardial tissue between the AP39 control group and the Control group.

3.5. AP39 inhibits excessive mitochondrial autophagy through the PINK1/Parkin pathway in cardiomyocytes

H9c2 cells were treated with CoCl₂ (0, 200, 400, 600, 800, 1000, 1200 μ M) and changes in cell viability were measured using the CCK8 assay (Fig. 4A). H9c2 cells treated with 800 μ M CoCl₂ were selected to establish a model of myocardial cell hypoxic injury.

Simultaneously, mitochondrial hydrogen sulfide (H₂S) levels in cardiomyocytes were detected using a mitochondrial H₂S fluorescence probe (Fig. 4D). The results showed significantly enhanced red fluorescence and weakened green fluorescence in the CoCl₂ group, indicating a decrease in mitochondrial H₂S levels ($P < 0.05$). Treatment with AP39 resulted in reduced red fluorescence and increased green fluorescence, indicating a significant increase in mitochondrial H₂S levels ($P < 0.05$). Conversely, treatment with the endogenous H₂S synthesis inhibitor PAG significantly decreased mitochondrial H₂S levels ($P < 0.05$). Western blot analysis was performed to evaluate the expression of endogenous hydrogen sulfide synthase CSE in cardiomyocytes (Fig. 4B, C). The results showed that CSE protein expression levels were significantly decreased in the CoCl₂ group ($P < 0.05$), while the intervention with AP39 significantly upregulated CSE protein



Fig. 2. Rat echocardiographic images in different groups.

Table 3

Comparison of cardiac ultrasound results in rats across different groups (mean ±SD).

Groups	LVEDD (mm)	LVESD (mm)	LVFS (%)
Control	4.315 ± 0.428	2.220 ± 0.136	48.210 ± 4.306
ISO	6.806 ± 0.306*	3.986 ± 0.307*	41.450 ± 3.408*
AP39 +ISO	5.441 ± 0.428 [#]	2.245 ± 0.256 [#]	58.697 ± 3.708 [#]
AP39 +ISO+PAG	6.956 ± 0.188 ^S	4.037 ± 0.217 ^S	41.950 ± 3.003 ^S
AP39	5.618 ± 0.503	2.271 ± 0.414	59.545 ± 6.428

Note : *P < 0.05 vs Control; [#]P < 0.05 vs ISO ; ^SP < 0.05 vs AP39 +ISO.

expression levels ($P < 0.05$). This effect of AP39 was reversed by the endogenous H₂S synthesis inhibitor PAG ($P < 0.05$). No statistically significant differences were observed between the AP39 control group

and the Control group ($P > 0.05$).

The levels of reactive oxygen species (ROS) in cardiomyocytes were measured using a ROS fluorescence detection kit (Fig. 4D). The results showed that the green fluorescence intensity in the CoCl₂ group was significantly higher than that in the Control group, indicating significantly elevated ROS levels compared to the Control group ($P < 0.05$). Treatment with AP39 resulted in a decrease in green fluorescence intensity, indicating a reduction in ROS levels ($P < 0.05$). This effect was reversed by PAG ($P < 0.05$).

Furthermore, changes in mitochondrial membrane potential in cardiomyocytes were assessed using a mitochondrial membrane potential assay kit (JC-1) (Fig. 4D). Compared to the Control group, cardiomyocytes in the CoCl₂ group exhibited increased green fluorescence and decreased red fluorescence, indicating a decrease in mitochondrial membrane potential. In contrast, the CoCl₂ +AP39 group showed

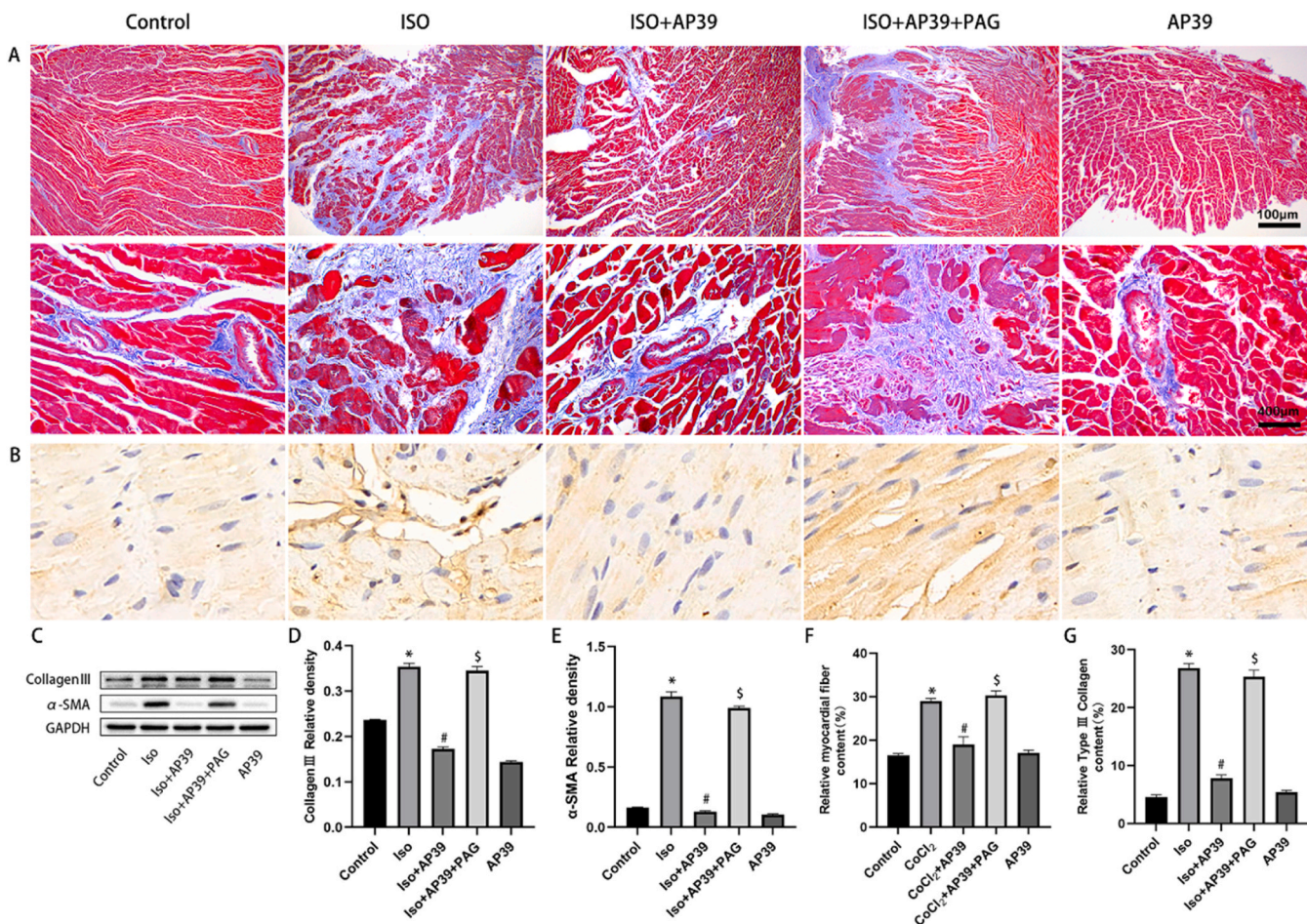


Fig. 3. AP39 improves myocardial fibrosis in rats with myocardial infarction. (A): Masson's staining of myocardial tissue in Control, ISO, ISO+AP39, ISO+AP39 +PAG, and AP39 groups of rats, 10 × 10 and 10 × 40 magnification (blue staining indicates collagen fibers), n = 3. (B): Immunohistochemical detection of Collagen III protein expression in myocardial tissue of each group of rats, 10 × 40 magnification, n = 3. (C-E): Western blot analysis of the expression changes of α-SMA and Collagen III in myocardial tissue of each group of rats. (F) Collagen volume fraction determined by Masson's staining. (G) Collagen III volume fraction determined by immunohistochemistry, n = 3, * P < 0.05 vs Control; [#]P < 0.05 vs ISO; ^SP < 0.05 vs ISO+AP39.

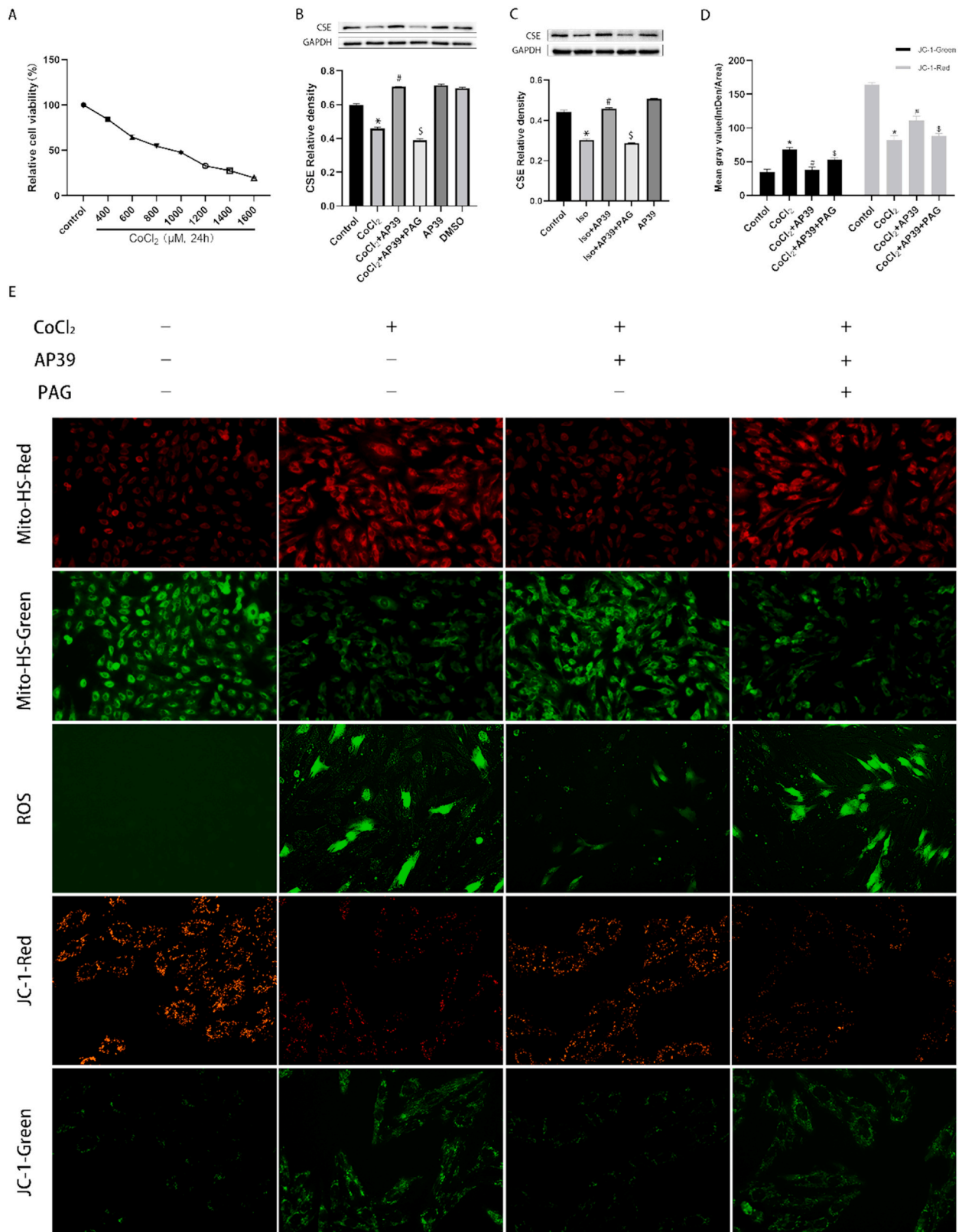


Fig. 4. AP39 increases CSE levels and mitochondrial membrane potential in myocardial tissue and cardiomyocytes of rats with myocardial infarction, while reducing ROS levels in cardiomyocytes. (A): Changes in the viability of H9c2 cardiomyocytes induced by different concentrations of CoCl₂ as measured by the CCK8 assay. (B): Western blot analysis of CSE expression in H9c2 cardiomyocytes. (C): Western blot analysis of CSE expression in myocardial tissue of different groups of rats. n = 3, * P < 0.05 vs Control; [#]P < 0.05 vs ISO; [§]P < 0.05 vs ISO+AP39. (D): Mean gray value (IntDen/Area) determined by JC-1, n = 3, * P < 0.05 vs Control; [#]P < 0.05 vs CoCl₂; [§]P < 0.05 vs CoCl₂ +AP39. (E) First and Second line: Detection of H₂S levels in mitochondria of H9c2 cardiomyocytes using a mitochondrial H₂S probe (Mito-HS); Third line: Detection of ROS levels in H9c2 cardiomyocytes using a ROS fluorescence probe; Fourth and Fifth line: Assessment of mitochondrial membrane potential changes in H9c2 cardiomyocytes using a mitochondrial membrane potential assay kit (JC-1).

decreased green fluorescence and increased red fluorescence compared to the CoCl_2 group, indicating an increase in mitochondrial membrane potential. Treatment with PAG reversed the effects of AP39.

RT-qPCR and Western blotting were performed to detect the mRNA and protein expression changes of mitochondrial autophagy-related proteins in cardiomyocytes of different groups. The RT-qPCR results (Fig. 5A, B) showed that compared to the Control group, the CoCl_2 group exhibited a significant increase in PINK1 mRNA levels in cardiomyocytes ($P < 0.05$). However, intervention with AP39 significantly reduced the mRNA expression levels of PINK1 compared to the CoCl_2 group ($P < 0.05$). The effect of AP39 in downregulating PINK1 was reversed by PAG treatment ($P < 0.05$). In addition, the CoCl_2 group showed a significant decrease in P62 mRNA expression levels compared to the Control group ($P < 0.05$). However, after AP39 intervention, the mRNA levels of P62 were significantly upregulated compared to the CoCl_2 group ($P < 0.05$). The effect of AP39 in upregulating P62 was reversed by PAG treatment ($P < 0.05$). The results of Western blotting (Fig. 5C-G) showed that compared to the Control group, the expression levels of PINK1, Parkin, and LC3-II/I proteins in cardiomyocytes of the CoCl_2 group were significantly increased ($P < 0.05$). Treatment with AP39 significantly downregulated the expression levels of these proteins ($P < 0.05$). However, the intervention of PAG significantly reversed the effect of AP39 in downregulating mitochondrial autophagy ($P < 0.05$). Furthermore, the expression levels of P62 protein in cardiomyocytes of the CoCl_2 group were significantly decreased compared to the Control group ($P < 0.05$). After AP39 treatment, the expression levels of P62 were significantly upregulated ($P < 0.05$), and this effect of AP39 was reversed by PAG treatment ($P < 0.05$).

At the same time, JC-1 detection kit was used to detect the changes of mitochondrial membrane potential in primary rat cardiomyocytes

(Figure6). Compared to the Control group, cardiomyocytes in the CoCl_2 group exhibited increased green fluorescence and decreased red fluorescence, indicating a decrease in mitochondrial membrane potential. In contrast, the $\text{CoCl}_2 + \text{AP39}$ group showed decreased green fluorescence and increased red fluorescence compared to the CoCl_2 group, indicating an increase in mitochondrial membrane potential. Treatment with PAG reversed the effects of AP39. No statistically significant differences were observed between the AP39 control group and the Control group ($P > 0.05$).

Immunofluorescence Staining were performed to detect the expression of PINK1 and Parkin in primary rat cardiomyocytes in each group (Figure6). The results showed that the fluorescence intensity of mitochondrial autophagy proteins PINK1 and Parkin in primary rat cardiomyocytes of CoCl_2 group was significantly increased. However, the fluorescence intensity of PINK1 and Parkin decreased after AP39 was applied. With the addition of PAG, the inhibitory effect of AP39 on mitochondrial autophagy was reversed. These results suggest that CoCl_2 -induced hypoxia injury in primary rat cardiomyocytes can lead to mitochondrial autophagy. The intervention of AP39 can reduce the mitochondrial autophagy of primary rat cardiomyocytes after hypoxia.

By using transmission electron microscopy, the mitochondrial structure and mitochondrial autophagy were observed in each group of rats (Fig. 6F). Compared to the Control group, the myocardial cells of rats in the ISO group showed blurred mitochondrial cristae and prominent vacuoles, indicating a higher presence of mitochondrial autophagosomes. In contrast to the ISO group, the AP39 + ISO group showed some improvement in the aforementioned features, but a noticeable decrease in the presence of mitochondrial autophagosomes in the field of view. When comparing the AP39 + ISO group to the AP39 + ISO + PAG group, the changes were similar to the ISO group, with evident

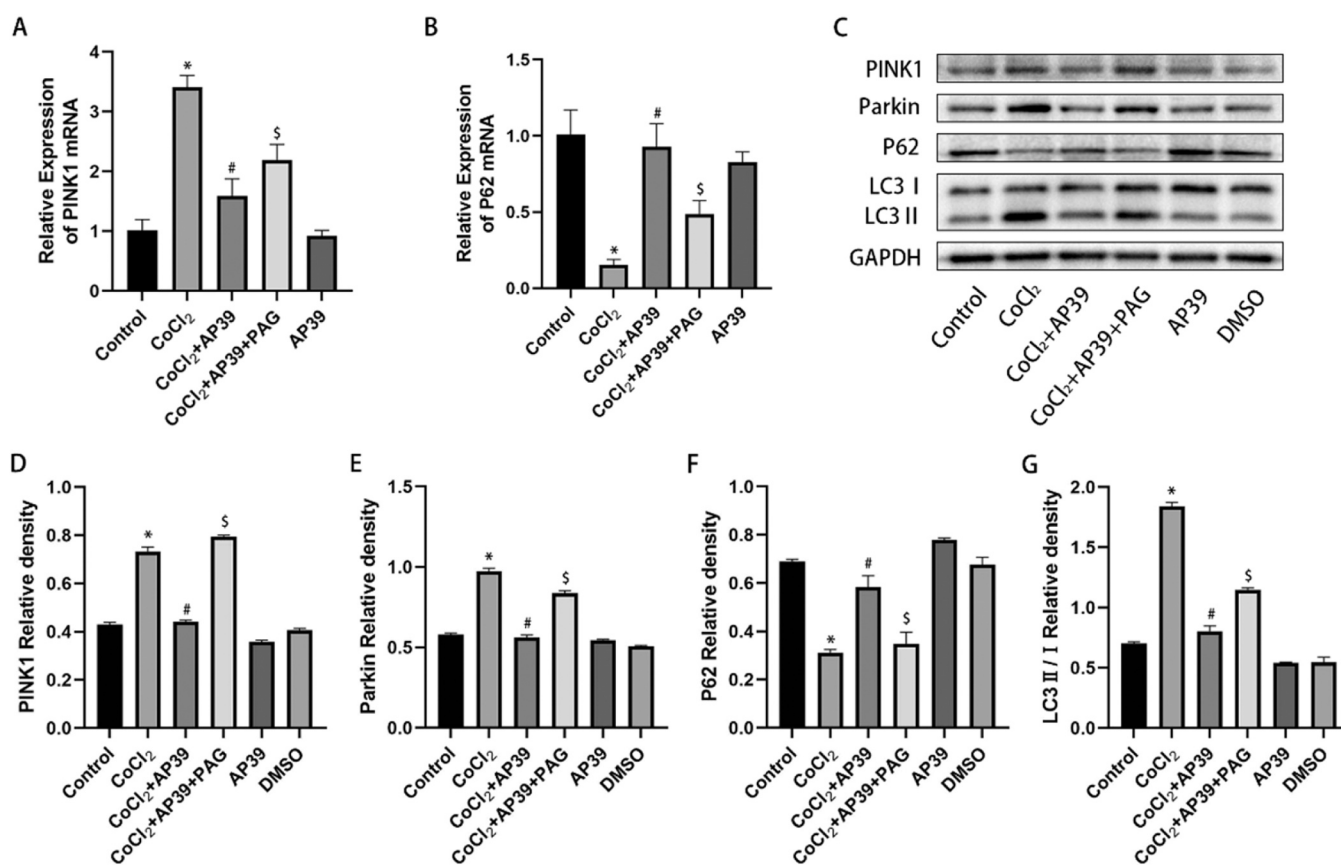


Fig. 5. AP39 inhibits mitochondrial autophagy in hypoxic H9c2 cardiomyocytes. (A-B): RT-qPCR analysis of PINK1 and P62 mRNA changes in H9c2 cardiomyocytes of each group. $n = 3$, * $P < 0.05$ vs Control; # $P < 0.05$ vs CoCl_2 ; \$ $P < 0.05$ vs $\text{CoCl}_2 + \text{AP39}$. (C-G): Western blot analysis of PINK1, Parkin, P62, and LC3 protein expression changes in H9c2 cardiomyocytes. $n = 3$, * $P < 0.05$ vs Control; # $P < 0.05$ vs CoCl_2 ; \$ $P < 0.05$ vs $\text{CoCl}_2 + \text{AP39}$.

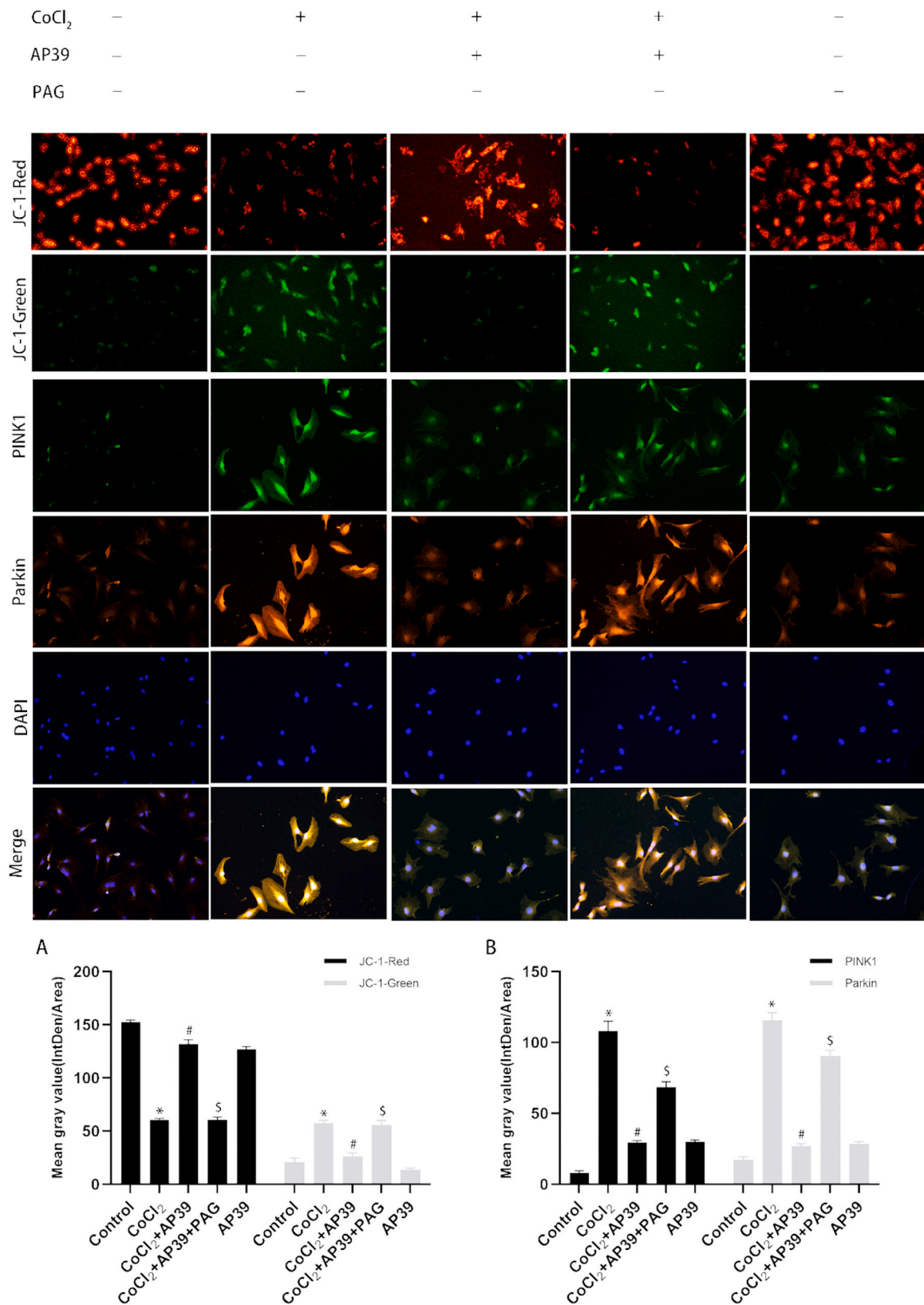


Fig. 6. AP39 increases mitochondrial membrane potential, while inhibiting the expression of PINK1 and Parkin in hypoxic primary rat cardiomyocytes. First and Second line: Assessment of mitochondrial membrane potential changes in primary rat cardiomyocytes using a mitochondrial membrane potential assay kit (JC-1). Third to Sixth line: The expression of PINK1 and Parkin in primary rat cardiomyocytes using Immunofluorescence Staining. (A-B): Mean gray value(IntDen/Area) determined by JC-1 and Immunofluorescence Staining, n = 3, *P < 0.05 vs Control; #P < 0.05 vs CoCl₂; \$P < 0.05 vs CoCl₂ +AP39.

mitochondrial autophagosomes.

Additionally, Western blot experiments were conducted to examine the expression levels of mitochondrial autophagy-related proteins (LC3, P62, PINK1, Parkin) in cardiac tissue. The results showed that compared to the Control group, the ISO group exhibited significant upregulation of LC3II/I, PINK1, and Parkin protein expression levels ($P < 0.05$), along with a significant downregulation of P62 expression level ($P < 0.05$).

However, after treatment with AP39, there was a significant down-regulation of LC3II/I, PINK1, and Parkin protein expression levels ($P < 0.05$), and a significant upregulation of P62 expression level ($P < 0.05$) in cardiac tissue. Furthermore, when the endogenous hydrogen sulfide synthesis enzyme CSE was inhibited by PAG, the changes in protein expression levels mentioned above were reversed (Fig. 7A-E).

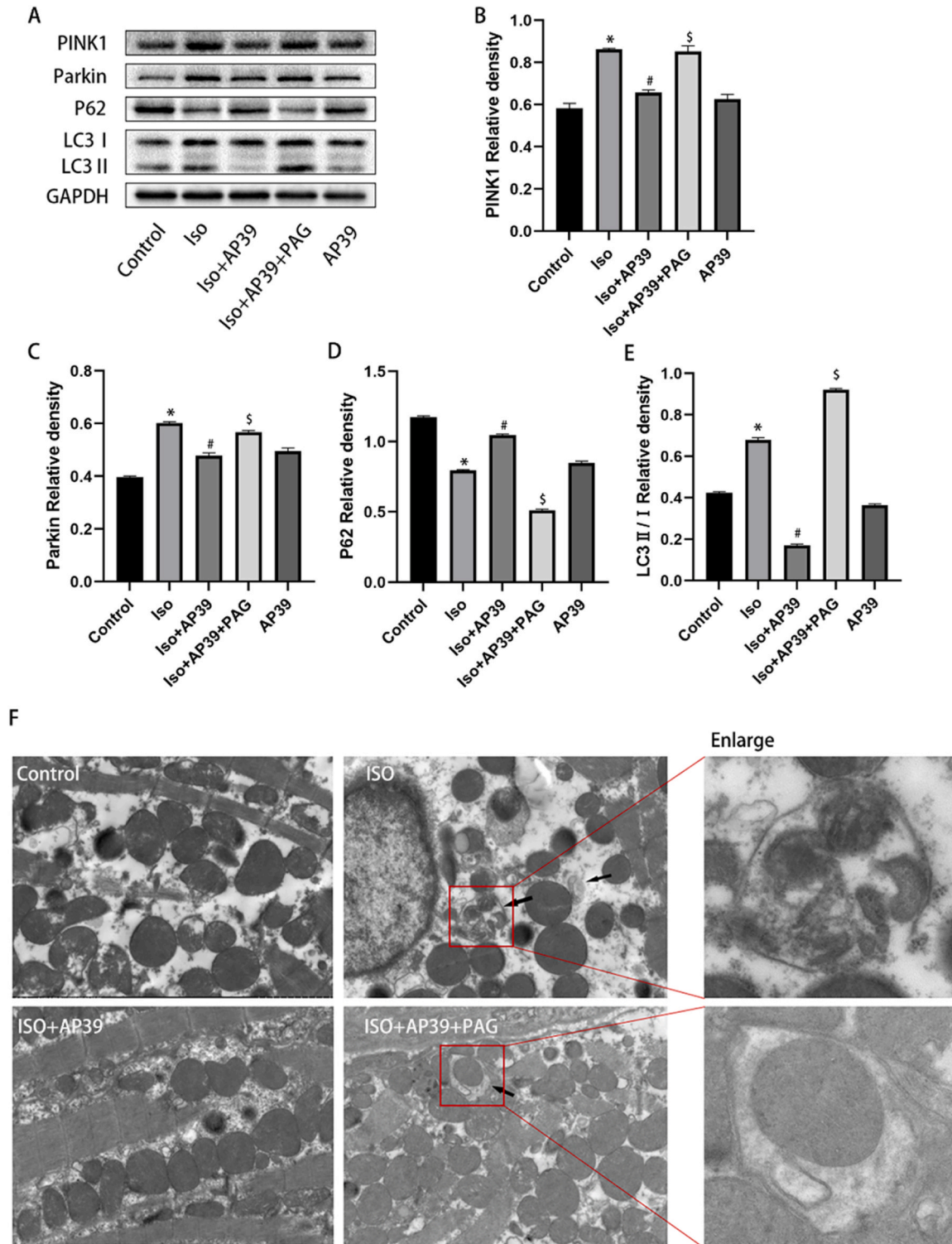


Fig. 7. AP39 inhibits mitochondrial autophagy in rat myocardial infarction heart tissue. (A-E): Western blot analysis of the expression changes of PINK1, Parkin, P62, and LC3 in rat myocardial tissue. $n = 3$, * $P < 0.05$ vs Control; # $P < 0.05$ vs ISO; \$ $P < 0.05$ vs ISO+AP39. (F): Transmission electron microscopy observation of mitochondrial morphology and mitochondrial autophagy in rat myocardial infarction heart tissue.

3.6. AP39 can inhibit myocardial cell ferroptosis by suppressing excessive mitochondrial autophagy

The protein expression levels of GPX4 and SLC7a11 in rat myocardial tissue were assessed by Western blot analysis (Fig. 8A-C). The results showed that compared to the Control group, the expression levels of GPX4 and SLC7a11 were significantly decreased in the ISO group ($P < 0.05$). Treatment with AP39 significantly upregulated the expression levels of GPX4 and SLC7a11 ($P < 0.05$). However, after treatment with PAG, the effect of AP39 in upregulating these proteins was reversed, and the expression levels of GPX4 and SLC7a11 were significantly decreased ($P < 0.05$). There was no significant statistical difference between the AP39 control group and the Control group ($P > 0.05$).

In this study, the mRNA and protein expression levels of GPX4 and SLC7a11 in H9c2 myocardial cells were examined using RT-qPCR and Western blot analysis. The RT-qPCR results showed that the mRNA levels of GPX4 and SLC7a11 were significantly decreased in myocardial cells induced by CoCl₂-induced hypoxia ($P < 0.05$). Treatment with AP39 in hypoxic myocardial cells resulted in a significant increase in the mRNA levels of GPX4 and SLC7a11 ($P < 0.05$). However, after treatment with PAG, the effect of AP39 in upregulating GPX4 and SLC7a11 mRNA was reversed ($P < 0.05$). There was no significant statistical difference between the AP39 control group and the Control group ($P > 0.05$) (Fig. 7G, H). The Western blotting results showed that the protein expression levels of GPX4 and SLC7a11 were significantly decreased in myocardial cells induced by CoCl₂-induced hypoxia ($P < 0.05$). Treatment with AP39 in hypoxic myocardial cells led to a significant increase in the expression levels of GPX4 and SLC7a11 ($P < 0.05$). However, after treatment with PAG, the effect of AP39 in upregulating GPX4 and SLC7a11 protein expression was reversed ($P < 0.05$). There was no significant statistical difference between the AP39 control group and the Control group ($P > 0.05$) (Fig. 8D-F).

The content of Fe²⁺ in myocardial mitochondria was assessed using the mitochondrial Fe²⁺ fluorescent probe (mito-ferrogreen) (Fig. 8I). The CoCl₂ group exhibited strong green fluorescence ($P < 0.05$), indicating a higher level of free iron ions in myocardial cells. Treatment with AP39 significantly reduced the green fluorescence ($P < 0.05$), suggesting a decrease in the content of free iron ions in myocardial cells. However, after treatment with PAG, the green fluorescence significantly increased ($P < 0.05$), indicating a significant increase in the content of Fe²⁺ in myocardial cells after inhibiting endogenous hydrogen sulfide synthesis.

In order to investigate whether AP39 can antagonize myocardial ferroptosis by inhibiting mitochondrial autophagy, the CoCl₂ + AP39 + CCCP group was established, where CCCP is a mitochondrial autophagy inducer that activates the PINK1/Parkin pathway [11]. Western blotting was performed to examine the protein expression changes of GPX4 and SLC7a11 in H9c2 myocardial cells (Fig. 9). The results showed that compared to the Control group, the expression levels of GPX4 and SLC7a11 were significantly decreased in the CoCl₂ group ($P < 0.05$). In the CoCl₂ + AP39 group, the expression levels of GPX4 and SLC7a11 in myocardial cells were significantly upregulated ($P < 0.05$). However, upon activation of mitochondrial autophagy by CCCP, the expression levels of GPX4 and SLC7a11 in myocardial cells were significantly downregulated ($P < 0.05$). There was no statistically significant difference in the expression of the above proteins between the AP39 control group, the DMSO group (solvent control), and the Control group ($P > 0.05$).

The content of Fe²⁺ in myocardial cell mitochondria was measured using the mitochondrial Fe²⁺ fluorescence probe (Mito-FerroGreen). The CoCl₂ group exhibited strong green fluorescence ($P < 0.05$), indicating a higher level of free iron ions in myocardial cells. After intervention with AP39, the green fluorescence significantly decreased ($P < 0.05$), suggesting a reduction in the content of free iron ions in myocardial cells. However, upon activation of mitochondrial autophagy with CCCP, the green fluorescence in myocardial cells significantly

increased ($P < 0.05$), indicating a significant increase in the content of Fe²⁺ in myocardial cells ($P < 0.05$) (Fig. 8I).

3.7. AP39 can downregulate the expression of fibrosis-related proteins in hypoxic myocardial cells by inhibiting ferroptosis

The expression levels of myocardial fibrosis-related proteins (Collagen I, TGF-β, and α-SMA) in myocardial cells were measured using Western blotting (Fig. 10). The results showed that compared to the Control group, the protein expression levels of Collagen I, TGF-β, and α-SMA were significantly increased in the CoCl₂ group ($P < 0.05$). Treatment with AP39 significantly downregulated the elevated expression of fibrosis-related proteins in hypoxic myocardial cells ($P < 0.05$). However, when the ferroptosis inducer RSL3 was used for intervention, the effect of AP39 in downregulating the protein expression levels of Collagen I, TGF-β, and α-SMA in hypoxic myocardial cells was significantly reversed ($P < 0.05$). There was no statistically significant difference in protein expression between the AP39 control group, the DMSO group (solvent control), and the Control group ($P > 0.05$).

4. Discussion

In this study, we constructed *in vivo* and *in vitro* models of myocardial infarction and myocardial cell hypoxic injury and administered the mitochondrial-targeted H₂S donor AP39. The aim was to elucidate the role and underlying regulatory mechanisms of mitochondrial-targeted H₂S in improving myocardial fibrosis after myocardial infarction. The results of this study revealed that the reconstruction of mitochondrial H₂S homeostasis by the mitochondrial-targeted H₂S donor AP39 improved myocardial fibrosis after myocardial infarction, and this effect was associated with the inhibition of PINK1/Parkin-mediated mitochondrial autophagy and antagonism of ferroptosis in myocardial cells. This study will provide new therapeutic strategies for preventing and treating myocardial fibrosis after myocardial infarction, as well as a new theoretical basis for the reconstruction of mitochondrial H₂S homeostasis by mitochondrial-targeted H₂S in antagonizing myocardial fibrosis after myocardial infarction.

Myocardial infarction can lead to ischemic and hypoxic damage in myocardial cells. Adult mammalian myocardial cells have almost no regenerative capacity, so the loss of a large number of myocardial cells can trigger a fibrotic repair program, resulting in excessive deposition of collagen fiber tissue in the interstitium, ultimately replacing necrotic myocardial tissue with excessive fibrous tissue [30]. Antagonizing the injury and death of hypoxic myocardial cells is currently an important strategy for improving post-infarction myocardial fibrosis. This study found that myocardial fibrosis occurred in the myocardial tissue of rats with isoproterenol-induced myocardial infarction and was associated with a downregulation of endogenous H₂S levels leading to mitochondrial H₂S instability in the injured myocardium. This study revealed that myocardial tissue and hypoxic cardiomyocytes in rats exhibited a significant decrease in hydrogen sulfide (H₂S) levels within the mitochondria following myocardial infarction. The expression of endogenous hydrogen sulfide-generating enzyme, cystathionine gamma-lyase (CSE), was also reduced. However, administration of the mitochondria-targeted H₂S donor, AP39, restored the mitochondrial H₂S homeostasis. Previous studies have shown that exogenous H₂S can inhibit the production of interstitial collagen fibers and antagonize diabetic and alcohol-induced myocardial fibrosis [31,32]. Our research group has previously found that H₂S can improve doxorubicin-induced myocardial fibrosis [33]. In this study, we found that the mitochondrial-targeted H₂S donor AP39 significantly improved myocardial fibrosis in rats with myocardial infarction and improved cardiac function. Therefore, post-infarction myocardial injury and cardiac fibrosis are associated with the downregulation of endogenous H₂S, and AP39 can reconstruct mitochondrial H₂S homeostasis to improve myocardial fibrosis after myocardial infarction and antagonize

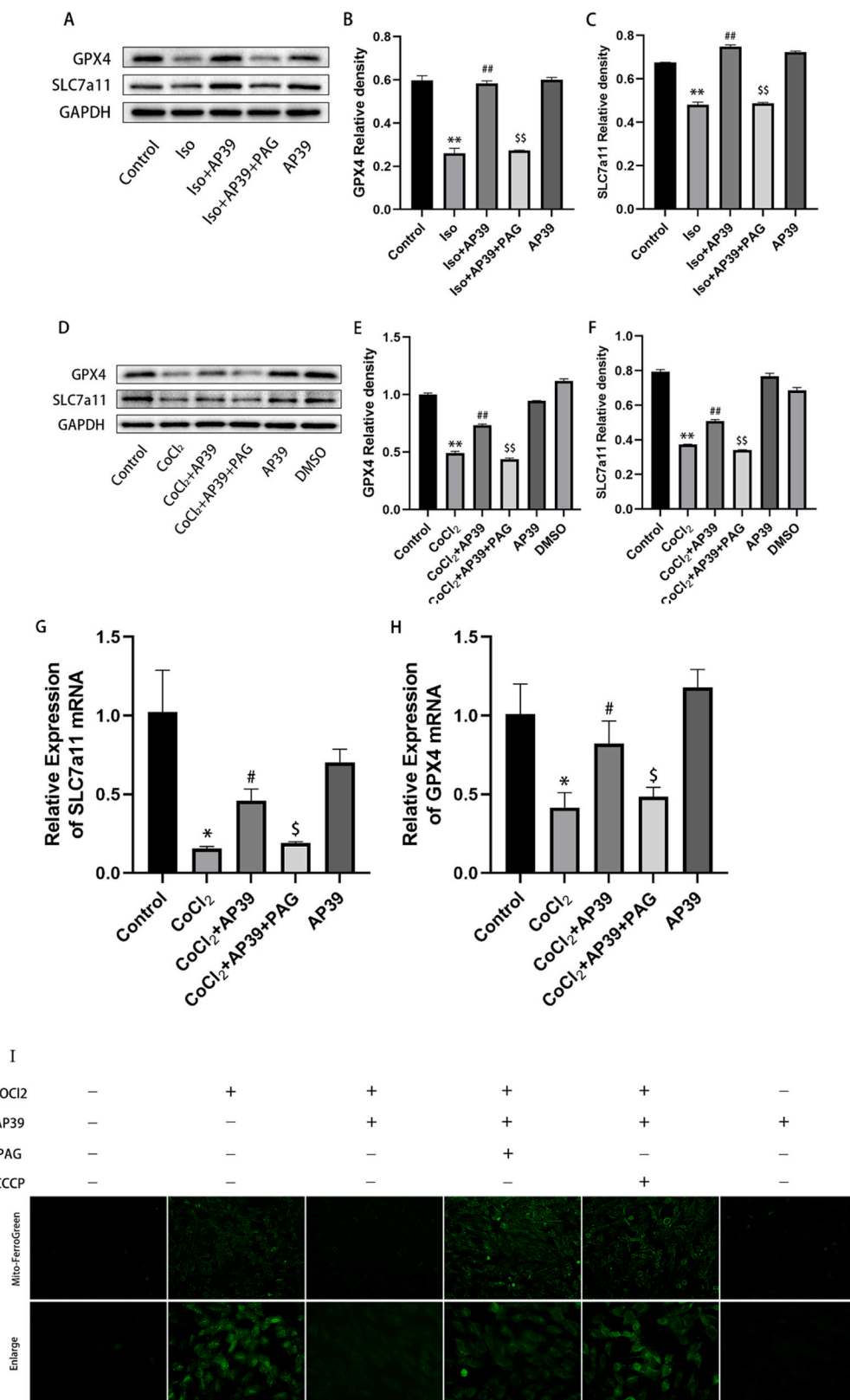


Fig. 8. AP39 inhibits myocardial ferroptosis in rat myocardial tissue and CoCl₂-induced hypoxic damage in H9c2 myocardial cells. (A-C): Western blot analysis of the expression changes of GPX4 and SLC7a11 in rat myocardial tissue. n = 3, * P < 0.05 vs Control; #P < 0.05 vs ISO; §P < 0.05 vs ISO+AP39. (D-F): Western blot analysis of the expression changes of GPX4 and SLC7a11 in H9c2 myocardial cells. n = 3, * P < 0.05 vs Control; #P < 0.05 vs CoCl₂; §P < 0.05 vs CoCl₂ +AP39. (G-H): RT-qPCR analysis of the mRNA level changes of GPX4 and SLC7a11 in H9c2 myocardial cells. n = 3, * P < 0.05 vs Control; #P < 0.05 vs CoCl₂; §P < 0.05 vs CoCl₂ +AP39. (I): Detection of changes in the content of free Fe²⁺ in myocardial cell mitochondria using the mitochondrial Fe²⁺ fluorescent probe (Mito-FerroGreen).

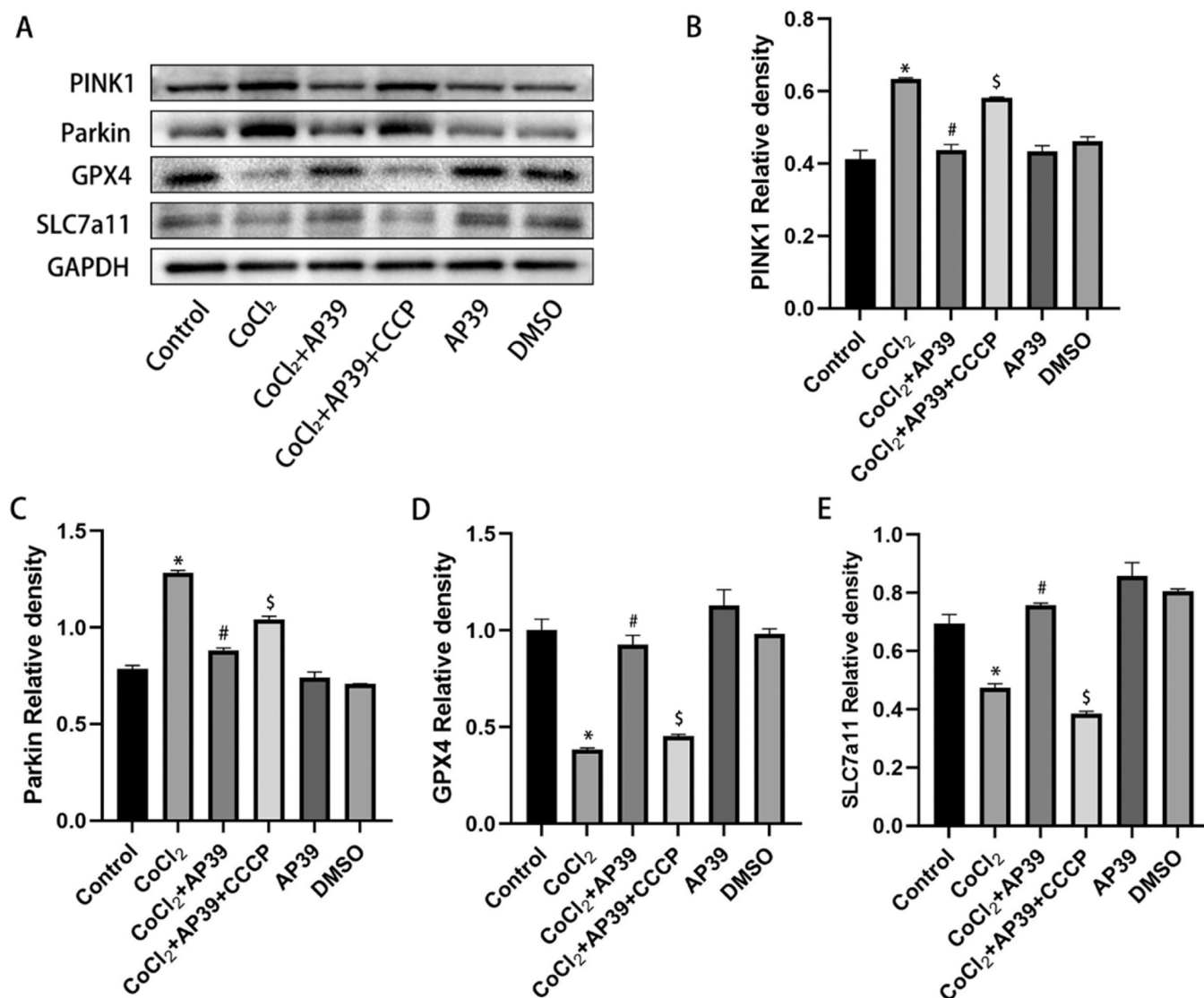


Fig. 9. AP39 can antagonize ferroptosis in hypoxic myocardial cells by inhibiting mitochondrial autophagy through the PINK1/Parkin pathway. (A-E): Western blot analysis of the expression changes of PINK1, Parkin, GPX4, and SLC7a11 in H9c2 myocardial cells. $n = 3$, * $P < 0.05$ vs Control; # $P < 0.05$ vs CoCl₂; § $P < 0.05$ vs CoCl₂ + AP39.

pathological cardiac remodeling.

Mitophagy is a cellular process where dysfunctional mitochondria are selectively eliminated through self-degradation, providing nutrients to healthy organelles. Mitochondria are vital for ATP production. Excessive activation of mitochondrial autophagy leads to the complete clearance of mitochondria within the cell, resulting in impaired ATP synthesis. This is detrimental to the heart, which relies heavily on mitochondrial energy for maintaining contractile function [34]. Studies have found that inhibiting excessive activation of mitochondrial autophagy in a rat model of cardiac ischemia-reperfusion can effectively reduce ischemia-reperfusion injury and decrease myocardial infarction area. Furthermore, it has been discovered that supplementation of H₂S can reduce mitochondrial fission and mitochondrial autophagy in skeletal muscle cells, improving interstitial fibrosis and function in skeletal muscle associated with hyperhomocysteinemia [35]. Excessive activation of mitophagy leads to mitochondrial depletion, impaired clearance of harmful metabolites, elevated levels of reactive oxygen species (ROS) [36–38]. Accumulation of free iron in the solvent triggers the Fenton reaction [39], ultimately leading to cellular ferroptosis. Inhibition of ferritinophagy and mitophagy by downregulating NCOA4 and PINK1 blocks ferroptosis [40]. The PINK1-Parkin pathway is a key regulatory

pathway of mitophagy. When mitochondria are damaged, the inner mitochondrial membrane depolarizes. PINK1 with kinase activity on the outer mitochondrial membrane recruits Parkin to the mitochondrial surface, activating mitophagy. Research has found that roloxifene can inhibit inflammation-induced mitophagy, downregulate the expression of PINK1 and Parkin, reduce ROS generation, and slow down the development of myocardial hypertrophy and heart failure [41]. However, the relationship between PINK1/Parkin-mediated mitophagy and ferroptosis in myocardial infarction is not fully understood. Our research findings also revealed that administration of AP39 resulted in a reduction in mitochondrial autophagosomes, an increase in mitochondrial membrane potential, a decrease in oxidative stress, and a decrease in the expression of proteins and RNA related to mitochondrial autophagy and ferroptosis in myocardial tissue of myocardial infarction rats. However, these effects of AP39 were reversed when PAG was administered. These results indicate that PINK1/Parkin-mediated mitophagy is elevated during myocardial infarction, and the mitochondria-targeted H₂S donor AP39 can inhibit mitophagy, restore mitochondrial membrane potential, reduce ROS generation, and prevent ferroptosis in cardiac myocytes.

Ferroptosis is a form of non-apoptotic cell death characterized by the

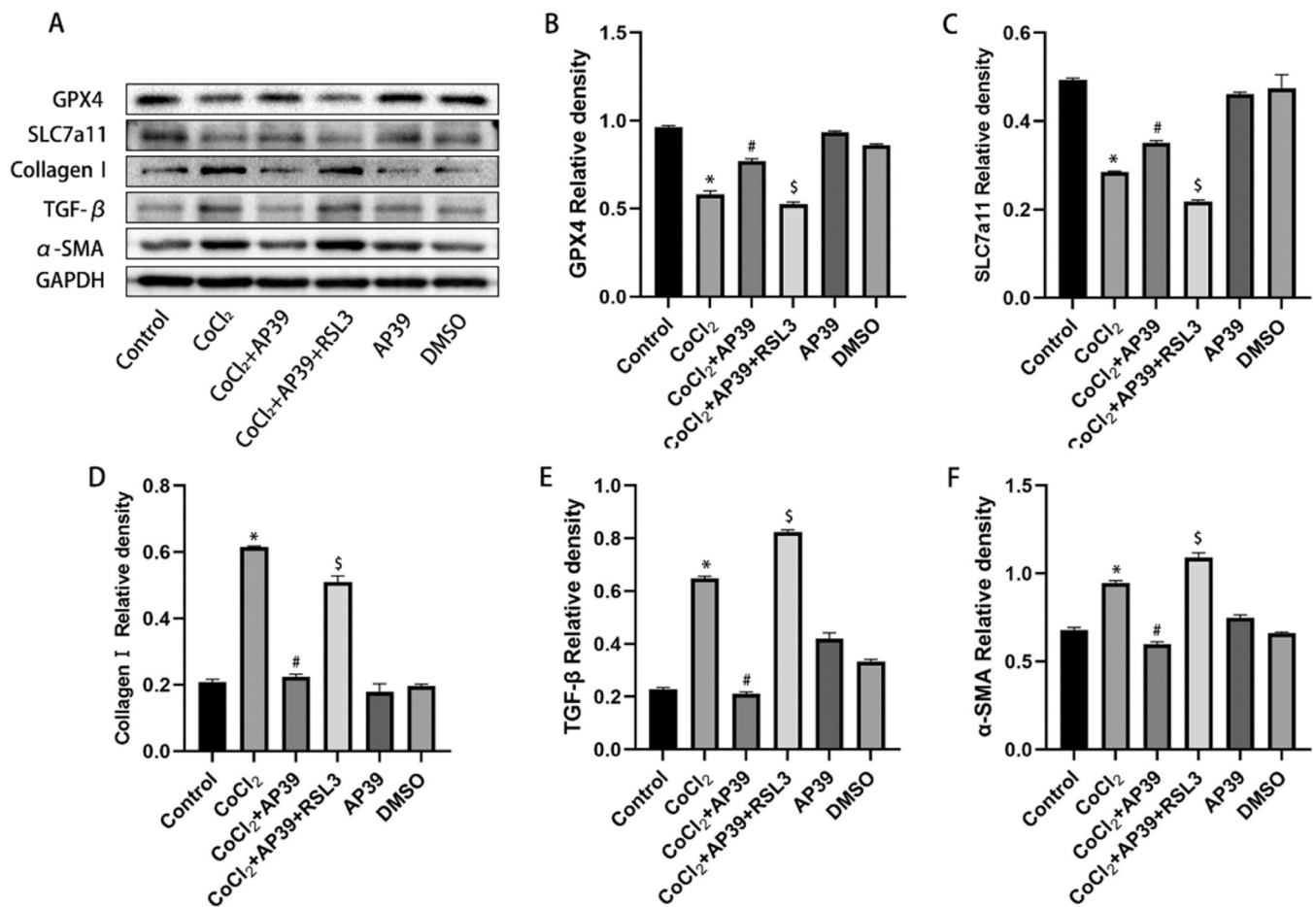


Fig. 10. AP39 inhibits ferroptosis and downregulates the expression of fibrosis-related proteins in hypoxic myocardial cells. (A-F): Western blot analysis of the expression changes of GPX4, SLC7a11, Collagen I, TGF- β , and α -SMA in H9c2 myocardial cells. $n = 3$, * $P < 0.05$ vs Control; # $P < 0.05$ vs CoCl₂; $^{\S}P < 0.05$ vs CoCl₂ + AP39.

accumulation of intracellular iron, which leads to increased levels of toxic lipid peroxides and reactive oxygen species (ROS). When iron metabolism is disrupted, the excess free iron participates in the Fenton reaction, resulting in ROS production and membrane lipid damage, ultimately leading to cell death through iron-dependent mechanisms [13]. Studies have found increased expression of iron homeostasis-regulating peptides in ischemic myocardial tissue and reduced apoptosis and necrosis in the infarcted myocardium [42]. Studies have found that myocardial cells accumulated more iron ions in the mitochondria under hypoxic conditions. The key step in cellular ferroptosis, the Fenton reaction, can be inhibited by the essential intracellular antioxidant glutathione. The deficiency and impairment of intracellular glutathione mediate cellular ferroptosis [18]. The results of our study also showed treatment with the mitochondrial-targeted H₂S donor AP39 reduced the accumulation of iron ions in hypoxic myocardial cells and the expression of important regulatory factors GPX4 and SLC7A11, which antagonize ferroptosis, was significantly upregulated in the body. Other studies have found that exogenous H₂S enhances endogenous H₂S synthesis enzymes, promotes the generation of endogenous H₂S, regulates iron metabolism, reduces oxidative stress levels in myocardial cells, inhibits ferroptosis, and protects cardiac function in aging rats [43]. Our research found that AP39 can inhibit PINK1/Parkin-mediated mitochondrial autophagy, restore mitochondrial membrane potential, reduce ROS generation, and thus inhibit ferroptosis in myocardial cells. In addition, studies have found that transferrin receptor (TFRC) increases intracellular iron content, mediates ROS release, activates mitochondrial autophagy, and further promotes cellular ferroptosis

[37]. Mitochondrial iron-binding protein FiMt induces mitochondrial autophagy through the ROS/PINK1/Parkin pathway, promoting ferroptosis in osteoblasts [36]. In our study, when the mitochondrial autophagy inducer CCCP was administered concurrently with AP39, an increase in PINK1/Parkin-mediated mitochondrial autophagy was observed, and mitochondrial iron accumulation in myocardial cells occurred. The aforementioned effects of AP39 were reversed. Research has shown that inhibiting ferroptosis can effectively reduce myocardial injury, decrease the expression of fibrosis-related proteins (collagen I and α -SMA) in rat myocardium [44], and reduce cardiac damage in ischemia-reperfusion mice, alleviating cardiac inflammation and fibrosis [45]. When AP39 was administered concurrently with the PAG, an increase in PINK1/Parkin-mediated mitochondrial autophagy was observed, along with an increase in ferroptosis-related protein expression and aggravation of myocardial fibrosis. The beneficial effects of AP39 on collagen production in hypoxic myocardial cells were reversed when ferroptosis was activated by RSL3. The above research results suggest that the mitochondrial-targeted H₂S donor AP39 can inhibit PINK1/Parkin-mediated mitochondrial autophagy, alleviate mitochondrial damage in myocardial cells after myocardial infarction, restore impaired mitochondrial membrane potential, reduce ROS generation, and inhibit ferroptosis in myocardial cells. This may represent an important target for the improvement of myocardial fibrosis after myocardial infarction by exogenous mitochondrial-targeted H₂S.

In summary, we have discovered that the mitochondrial-targeted H₂S donor AP39 can inhibit excessive mitochondrial autophagy through the PINK1/Parkin pathway, counteracting ferroptosis in

myocardial cells and improving myocardial fibrosis in rats with myocardial infarction. Restoring mitochondrial H₂S homeostasis may represent a novel strategy for combating hypoxic myocardial injury and myocardial fibrosis after infarction. In this study, we found that the mitochondrial-targeted H₂S donor AP39 can improve myocardial fibrosis in rats with myocardial infarction. Our results also revealed that excessive mitochondrial autophagy mediated by the PINK1/Parkin pathway leads to mitochondrial depletion and triggers ferroptosis in myocardial cells. This process may be one of the important mechanisms underlying myocardial fibrosis after myocardial infarction, and it suggests that targeting excessive mitochondrial autophagy through the PINK1/Parkin pathway to counteract ferroptosis in myocardial cells may serve as a novel therapeutic target for preventing and treating myocardial fibrosis after myocardial infarction. Therefore, this study has identified a new mechanism for the anti-myocardial fibrosis effects of mitochondrial-targeted H₂S and provides new insights for the prevention and treatment of myocardial fibrosis and myocardial remodeling after myocardial infarction.

Funding statement

This project was supported by the National Natural Science Foundation of China (No. 82074236 and No. 81870230), Clinical Major Projects of Hunan Provincial Health Commission (No. 20201913), the Natural Science Foundation of Hunan Province (No. 2021JJ70035, No. 2021JJ40499 and No. 2021JJ70116).

CRedit authorship contribution statement

Ting Yang: Conceptualization, Preparation, Methodology, Data curation, Formal analysis, Visualization, Writing – original draft. **Qi Yang:** Conceptualization, Preparation, Methodology, Data curation, Formal analysis, Writing – original draft. **Qi Lai:** Preparation, Formal analysis. **Junxiong Zhao:** Preparation, Formal analysis. **Liangui Nie:** Formal analysis, Funding acquisition. **Shengquan Liu:** Formal analysis. **Jun Yang:** Conceptualization, Project administration, Funding acquisition, Supervision, Formal analysis. **Chun Chu:** Conceptualization, Project administration, Supervision, Funding acquisition, Resources, Validation, Writing – review & editing.

Declaration of Competing Interest

The authors declare no conflicts of interest.

Data availability

Data will be made available on request.

Acknowledgements

None.

Data avail ability statement

Data available on request from the authors. The data that support the findings of this study are available from the corresponding author upon reasonable request. Some data may not be made available because of privacy or ethical restrictions.

References

- [1] 《中国心血管健康与疾病报告》2021 (冠心病部分内容) [J]. 心肺血管病杂志, 2022, 41(12): 1205–1211. doi.org/10.3969/j.issn.1007-5062.2022.07.001.
- [2] L. Xu, C.C. Yates, P. Lockyer, L. Xie, A. Bevilacqua, J. He, C. Lander, C. Patterson, M. Willis, MMI-0100 inhibits cardiac fibrosis in myocardial infarction by direct actions on cardiomyocytes and fibroblasts via MK2 inhibition[J], *J. Mol. Cell Cardiol.* 77 (2014) 86–101, <https://doi.org/10.1016/j.yjmcc.2014.09.011>.
- [3] X. Jin, C. Chen, D. Li, Q. Su, Y. Hang, P. Zhang, W. Hu, PRDX2 in Myocyte Hypertrophy and Survival is Mediated by TLR4 in Acute Infarcted Myocardium, *J. I. Sci. Rep.* 7 (1) (2017) 6970, <https://doi.org/10.1038/s41598-017-06718-7>.
- [4] F. Yang, Y. Qin, J. Lv, Y. Wang, H. Che, X. Chen, Y. Jiang, A. Li, X. Sun, E. Yue, L. Ren, Y. Li, Y. Bai, L. Wang, Silencing long non-coding RNA Kcnq1ot1 alleviates pyroptosis and fibrosis in diabetic cardiomyopathy[J], *Cell Death Dis.* 9 (10) (2018) 1000, <https://doi.org/10.1038/s41419-018-1029-4>.
- [5] D.A. Chistiakov, T.P. Shkurat, A.A. Melnichenko, A.V. Grechko, A.N. Orekhov, The role of mitochondrial dysfunction in cardiovascular disease: a brief review[J], *Ann. Med.* 50 (2) (2018) 121–127, <https://doi.org/10.1080/07853890.2017.1417631>.
- [6] S. Jiang, J. Sun, N. Mohammadursun, Z. Hu, Q. Li, Z. Zhao, H. Zhang, J. Dong, Dual role of autophagy/mitophagy in chronic obstructive pulmonary disease[J], *Pulm. Pharm. Ther.* 56 (2019) 116–125, <https://doi.org/10.1016/j.pupt.2019.04.002>.
- [7] R.Y. Shi, S.H. Zhu, V. Li, S.B. Gibson, X.S. Xu, J.M. Kong, BNIP3 interacting with LC3 triggers excessive mitophagy in delayed neuronal death in stroke[J], *CNS Neurosci. Ther.* 20 (12) (2014) 1045–1055, <https://doi.org/10.1111/cns.12325>.
- [8] R. Shi, J. Weng, L. Zhao, X.M. Li, T.M. Gao, J. Kong, Excessive autophagy contributes to neuron death in cerebral ischemia[J], *CNS Neurosci. Ther.* 18 (3) (2012) 250–260, <https://doi.org/10.1111/j.1755-5949.2012.00295.x>.
- [9] N. Matsuda, S. Sato, K. Shiba, K. Okatsu, K. Saisho, C.A. Gautier, Y.S. Sou, S. Saiki, S. Kawajiri, F. Sato, M. Kimura, M. Komatsu, N. Hattori, K. Tanaka, PINK1 stabilized by mitochondrial depolarization recruits Parkin to damaged mitochondria and activates latent Parkin for mitophagy[J], *J. Cell Biol.* 189 (2) (2010) 211–221, <https://doi.org/10.1083/jcb.200910140>.
- [10] L.E. Fritsch, M.E. Moore, S.A. Sarraf, A.M. Pickrell, Ubiquitin and receptor-dependent mitophagy pathways and their implication in neurodegeneration[J], *J. Mol. Biol.* 432 (8) (2020) 2510–2524, <https://doi.org/10.1016/j.jmb.2019.10.015>.
- [11] C. Kondapalli, A. Kazlauskaitė, N. Zhang, H.I. Woodroof, D.G. Campbell, R. Gourlay, L. Burchell, H. Walden, T.J. Macartney, M. Deak, A. Knebel, D. Alessi, M.M. Muqit, PINK1 is activated by mitochondrial membrane potential depolarization and stimulates Parkin E3 ligase activity by phosphorylating Serine 65[J], *Open Biol.* 2 (5) (2012), 120080, <https://doi.org/10.1098/rsob.120080>.
- [12] S.H. Wang, X.L. Zhu, F. Wang, S.X. Chen, Z.T. Chen, Q. Qiu, W.H. Liu, M.X. Wu, B. Q. Deng, Y. Xie, J.T. Mai, Y. Yang, J.F. Wang, H.F. Zhang, Y.X. Chen, LncRNA H19 governs mitophagy and restores mitochondrial respiration in the heart through Pink1/Parkin signaling during obesity[J], *Cell Death Dis.* 12 (6) (2021) 557, <https://doi.org/10.1038/s41419-021-03821-6>.
- [13] S.J. Dixon, K.M. Lemberg, M.R. Lamprecht, R. Skouta, E.M. Zaitsev, C.E. Gleason, D.N. Patel, A.J. Bauer, A.M. Cantley, W.S. Yang, B. Morrison, 3rd, B.R. Stockwell, Ferroptosis: an iron-dependent form of nonapoptotic cell death[J], *Cell* 149 (5) (2012) 1060–1072, <https://doi.org/10.1016/j.cell.2012.03.042>.
- [14] T.J. Park, J.H. Park, G.S. Lee, J.Y. Lee, J.H. Shin, M.W. Kim, Y.S. Kim, J.Y. Kim, K. J. Oh, B.S. Han, W.K. Kim, Y. Ahn, J.H. Moon, J. Song, K.H. Bae, D.H. Kim, E. W. Lee, S.C. Lee, Quantitative proteomic analyses reveal that GPX4 downregulation during myocardial infarction contributes to ferroptosis in cardiomyocytes[J], *Cell Death Dis.* 10 (11) (2019) 835, <https://doi.org/10.1038/s41419-019-2061-8>.
- [15] Y. Song, B. Wang, X. Zhu, J. Hu, J. Sun, J. Xuan, Z. Ge, Human umbilical cord blood-derived MSCs exosome attenuate myocardial injury by inhibiting ferroptosis in acute myocardial infarction mice[J], *Cell Biol. Toxicol.* 37 (1) (2021) 51–64, <https://doi.org/10.1007/s10565-020-09530-8>.
- [16] Z. Zhang, J. Tang, J. Song, M. Xie, Y. Liu, Z. Dong, X. Liu, X. Li, M. Zhang, Y. Chen, H. Shi, J. Zhong, Elabela alleviates ferroptosis, myocardial remodeling, fibrosis and heart dysfunction in hypertensive mice by modulating the IL-6/STAT3/GPX4 signaling[J], *Free Radic. Biol. Med* 181 (2022) 130–142, <https://doi.org/10.1016/j.freeradbiomed.2022.01.020>.
- [17] D. Li, X. Liu, W. Pi, Y. Zhang, L. Yu, C. Xu, Z. Sun, J. Jiang, Fisetin attenuates doxorubicin-induced cardiomyopathy in vivo and in vitro by inhibiting ferroptosis through SIRT1/Nrf2 signaling pathway activation[J], *Front Pharm.* 12 (2021), 808480, <https://doi.org/10.3389/fphar.2021.808480>.
- [18] J. Liu, M. Zhang, C. Qin, Z. Wang, J. Chen, R. Wang, J. Hu, Q. Zou, X. Niu, Resveratrol attenuate myocardial injury by inhibiting ferroptosis via inducing KAT5/GPX4 in myocardial infarction. *J. J. Front Pharm.* 13 (2022), 906073, <https://doi.org/10.3389/fphar.2022.906073>.
- [19] Y. Zhuang, D. Yang, S. Shi, L. Wang, M. Yu, X. Meng, Y. Fan, R. Zhou, F. Wang, MiR-375-3p promotes cardiac fibrosis by regulating the ferroptosis mediated by GPX4[J], *Comput. Intell. Neurosci.* 2022 (2022) 9629158, <https://doi.org/10.1155/2022/9629158>.
- [20] Z. Li, H. Xia, T.E. Sharp, 3rd, K.B. Lapenna, A. Katsouda, J.W. Elrod, J. Pfeilschifter, K.F. Beck, S. Xu, M. Xian, T.T. Goodchild, A. Papapetropoulos, D.J. Lefter, Hydrogen sulfide modulates endothelial-mesenchymal transition in heart failure, *J. J. Circ. Res* 132 (2) (2023) 154–166, <https://doi.org/10.1161/CIRCRESAHA.122.321326>.
- [21] Y.D. Wen, H. Wang, Y.Z. Zhu, The drug developments of hydrogen sulfide on cardiovascular disease[J], *Oxid. Med Cell Longev.* 2018 (2018) 4010395, <https://doi.org/10.1155/2018/4010395>.
- [22] J.W. Calvert, W.A. Coetzee, D.J. Lefter, Novel insights into hydrogen sulfide-mediated cytoprotection[J], *Antioxid. Redox Signal* 12 (10) (2010) 1203–1217, <https://doi.org/10.1089/ars.2009.2882>.
- [23] M. Liu, Z. Li, B. Liang, L. Li, S. Liu, W. Tan, J. Long, F. Tang, C. Chu, J. Yang, Hydrogen sulfide ameliorates rat myocardial fibrosis induced by thyroxine through PI3K/AKT signaling pathway[J], *Endocr. J.* 65 (7) (2018) 769–781, <https://doi.org/10.1507/endocrj.EJ17-0445>.
- [24] Y. Li, M. Liu, X. Song, X. Zheng, J. Yi, D. Liu, S. Wang, C. Chu, J. Yang, Exogenous hydrogen sulfide ameliorates diabetic myocardial fibrosis by inhibiting cell aging

- through SIRT6/AMPK autophagy[J], *Front Pharm.* 11 (2020) 1150, <https://doi.org/10.3389/fphar.2020.01150>.
- [25] B. Szczesny, K. Modis, K. Yanagi, C. Coletta, S. Le Trionnaire, A. Perry, M.E. Wood, M. Whiteman, C. Szabo, AP39, a novel mitochondria-targeted hydrogen sulfide donor, stimulates cellular bioenergetics, exerts cytoprotective effects and protects against the loss of mitochondrial DNA integrity in oxidatively stressed endothelial cells in vitro[J], *Nitric Oxide* 41 (2014) 120–130, <https://doi.org/10.1016/j.niox.2014.04.008>.
- [26] M. Wepler, T. Merz, U. Wachter, J. Vogt, E. Calzia, A. Scheuerle, P. Moller, M. Groger, S. Kress, M. Fink, B. Lukaszewski, G. Rumm, B. Stahl, M. Georgieff, M. Huber-Lang, R. Torregrossa, M. Whiteman, O. Mccook, P. Radermacher, C. Hartmann, The Mitochondria-Targeted H₂S-Donor AP39 in a Murine Model of Combined Hemorrhagic Shock and Blunt Chest Trauma[J], *Shock* 52 (2) (2019) 230–239, <https://doi.org/10.1097/SHK.0000000000001210>.
- [27] Q.G. Karwi, J. Bornbaum, K. Boengler, R. Torregrossa, M. Whiteman, M.E. Wood, R. Schulz, G.F. Baxter, AP39, a mitochondria-targeting hydrogen sulfide (H₂S) donor, protects against myocardial reperfusion injury independently of salvage kinase signalling[J], *Br. J. Pharm.* 174 (4) (2017) 287–301, <https://doi.org/10.1111/bph.13688>.
- [28] C. Zheng, J.F. Lin, Z.H. Lin, W.Q. Lin, S. Thapa, Y.Z. Lin, H. Lian, Z.R. Liu, J. H. Chen, X.W. Li, Sodium houthuyfonate alleviates post-infarct remodeling in rats via AMP-activated protein kinase pathway[J], *Front Pharm.* 9 (2018) 1092, <https://doi.org/10.3389/fphar.2018.01092>.
- [29] Z. Fang, Z. Su, W. Qin, H. Li, B. Fang, W. Du, Q. Wu, B. Peng, P. Li, H. Yu, L. Li, W. Huang, Two-photon dual-channel fluorogenic probe for in situ imaging the mitochondrial H₂S/viscosity in the brain of drosophila Parkinson's disease model, *J. J. Chin. Chem. Lett.* 31 (11) (2020) 2903–2908, <https://doi.org/10.1016/j.ccllet.2020.03.063>.
- [30] N.G. Frangogiannis, Regulation of the inflammatory response in cardiac repair, *J. Circ. Res* 110 (1) (2012) 159–173, <https://doi.org/10.1161/CIRCRESAHA.111.243162>.
- [31] R. Yang, Q. Jia, S.F. Ma, Y. Wang, S. Mehmood, Y. Chen, Exogenous H₂S mitigates myocardial fibrosis in diabetic rats through suppression of the canonical Wnt pathway[J], *Int J. Mol. Med* 44 (2) (2019) 549–558, <https://doi.org/10.3892/ijmm.2019.4237>.
- [32] B. Liang, T. Xiao, J. Long, M. Liu, Z. Li, S. Liu, J. Yang, Hydrogen sulfide alleviates myocardial fibrosis in mice with alcoholic cardiomyopathy by downregulating autophagy[J], *Int J. Mol. Med* 40 (6) (2017) 1781–1791, <https://doi.org/10.3892/ijmm.2017.3191>.
- [33] Y. Li, T.P. Chandra, X. Song, L. Nie, M. Liu, J. Yi, X. Zheng, C. Chu, J. Yang, H₂S improves doxorubicin-induced myocardial fibrosis by inhibiting oxidative stress and apoptosis via Keap1-Nrf2[J], *Technol. Health Care* 29 (S1) (2021) 195–209, <https://doi.org/10.3233/THC-218020>.
- [34] R.E. Jimenez, D.A. Kubli, A.B. Gustafsson, Autophagy and mitophagy in the myocardium: therapeutic potential and concerns[J], *Br. J. Pharm.* 171 (8) (2014) 1907–1916, <https://doi.org/10.1111/bph.12477>.
- [35] M. Singh, S. Pushpakumar, Y. Zheng, R.P. Homme, I. Smolenkova, S.P. L. Mokshagundam, S.C. Tyagi, Hydrogen sulfide mitigates skeletal muscle mitophagy-led tissue remodeling via epigenetic regulation of the gene writer and eraser function[J], *Physiol. Rep.* 10 (16) (2022), e15422, <https://doi.org/10.14814/phy2.15422>.
- [36] X. Wang, H. Ma, J. Sun, T. Zheng, P. Zhao, H. Li, M. Yang, Mitochondrial ferritin deficiency promotes osteoblastic ferroptosis via mitophagy in type 2 diabetic osteoporosis[J], *Biol. Trace Elem. Res* 200 (1) (2022) 298–307, <https://doi.org/10.1007/s12011-021-02627-z>.
- [37] L. Zhang, F. Wang, D. Li, Y. Yan, H. Wang, Transferrin receptor-mediated reactive oxygen species promotes ferroptosis of KGN cells via regulating NADPH oxidase 1/PTEN induced kinase 1/acyl-CoA synthetase long chain family member 4 signaling [J], *Bioengineered* 12 (1) (2021) 4983–4994, <https://doi.org/10.1080/21655979.2021.1956403>.
- [38] X.Y. Song, P.C. Liu, W.W. Liu, J. Zhou, T. Hayashi, K. Mizuno, S. Hattori, H. Fujisaki, T. Ikejima, Silibinin inhibits ethanol- or acetaldehyde-induced ferroptosis in liver cell lines[J], *Toxicol. Vitro* 82 (2022), 105388, <https://doi.org/10.1016/j.tiv.2022.105388>.
- [39] P.K. Ziegler, J. Bollrath, C.K. Pallangyo, T. Matsutani, O. Canli, T. De Oliveira, M. A. Diamanti, N. Muller, J. Gamrekashvili, T. Putoczki, D. Horst, A.K. Mankan, M. G. Oner, S. Muller, J. Muller-Hocker, T. Kirchner, J. Slotta-Huspenina, M. M. Taketo, T. Reinheckel, S. Drose, A.C. Lerner, W.S. Wels, M. Ernst, T.F. Greten, M.C. Arkan, T. Korn, D. Wirth, F.R. Greten, Mitophagy in Intestinal Epithelial Cells Triggers Adaptive Immunity during Tumorigenesis[J], *Cell* 174 (1) (2018) 88–101 e16, <https://doi.org/10.1016/j.cell.2018.05.028>.
- [40] F. Yu, Q. Zhang, H. Liu, J. Liu, S. Yang, X. Luo, W. Liu, H. Zheng, Q. Liu, Y. Cui, G. Chen, Y. Li, X. Huang, X. Yan, J. Zhou, Q. Chen, Dynamic O-GlcNAcylation coordinates ferritinophagy and mitophagy to activate ferroptosis[J], *Cell Discov.* 8 (1) (2022) 40, <https://doi.org/10.1038/s41421-022-00390-6>.
- [41] S. Huo, W. Shi, H. Ma, D. Yan, P. Luo, J. Guo, C. Li, J. Lin, C. Zhang, S. Li, J. Lv, L. Lin, Alleviation of Inflammation and Oxidative Stress in Pressure Overload-Induced Cardiac Remodeling and Heart Failure via IL-6/STAT3 Inhibition by Raloxifene[J], *Oxid. Med Cell Longev.* 2021 (2021) 6699054, <https://doi.org/10.1155/2021/6699054>.
- [42] G. Simonis, K. Mueller, P. Schwarz, S. Wiedemann, G. Adler, R.H. Strasser, H. Kulaksiz, The iron-regulatory peptide hepcidin is upregulated in the ischemic and in the remote myocardium after myocardial infarction[J], *Peptides* 31 (9) (2010) 1786–1790, <https://doi.org/10.1016/j.peptides.2010.05.013>.
- [43] Z. Liang, Y. Miao, X. Teng, L. Xiao, Q. Guo, H. Xue, D. Tian, S. Jin, Y. Wu, Hydrogen sulfide inhibits ferroptosis in cardiomyocytes to protect cardiac function in aging rats[J], *Front Mol. Biosci.* 9 (2022), 947778, <https://doi.org/10.3389/fmolb.2022.947778>.
- [44] Z. Lv, F. Wang, X. Zhang, X. Zhang, J. Zhang, R. Liu, Etomidate attenuates the ferroptosis in myocardial ischemia/reperfusion rat model via Nrf2/HO-1 pathway [J], *Shock* 56 (3) (2021) 440–449, <https://doi.org/10.1097/SHK.0000000000001751>.
- [45] W. Cai, L. Liu, X. Shi, Y. Liu, J. Wang, X. Fang, Z. Chen, D. Ai, Y. Zhu, X. Zhang, Alox15/15-HpETE aggravates myocardial ischemia-reperfusion injury by promoting cardiomyocyte ferroptosis[J], *Circulation* 147 (19) (2023) 1444–1460, <https://doi.org/10.1161/CIRCULATIONAHA.122.060257>.